Longevity Greeks: What Should Insurers and Capital Market Investors Know About?

Kenneth Q. Zhou

Department of Statistics and Actuarial Science, University of Waterloo, Canada

Johnny S.-H. Li

Department of Statistics and Actuarial Science, University of Waterloo, Canada

Presented at the Living to 100 Symposium

Orlando, Fla.

January 4–6, 2017

Longevity Greeks:
What Should Insurers and Capital Market Investors Know About?

Kenneth Q. Zhou and Johnny S.-H. Li

Department of Statistics and Actuarial Science, University of Waterloo, Canada
E-mail: kenneth.zhou@uwaterloo.ca, shli@uwaterloo.ca

Abstract: Recently, it has been argued that capital markets may share some of the overwhelming longevity risk exposures borne by the pension and life insurance industries. The transfer of risk can be accomplished by trading standardized derivatives such as q-forwards that are linked to published mortality indexes. To strategize such trades, one may utilize "longevity Greeks," which are analogous to equity Greeks that have been used extensively in managing stock price risk. In this paper, we first derive three important longevity Greeks—delta, gamma and vega—on the basis of an extended version of the Lee-Carter model that incorporates stochastic volatility. We then study the properties of each longevity Greek and estimate the levels of effectiveness that different longevity Greek hedges can possibly achieve. The results reveal several interesting facts; for example, in a delta-vega hedge formed by q-forwards, the choice of reference ages does not materially affect hedge effectiveness, but the choice of times to maturity does. These facts may help insurers to better formulate their hedge portfolios, and issuers of mortality-linked securities to determine what security structures are more likely to attract liquidity.

1 Introduction

It has been argued that capital markets may share some of the overwhelming longevity risk exposures borne by the pension and life insurance industries (Graziani 2014; Michaelson and Mulholland 2014). Capital market investors may be interested in taking longevity risk in exchange for a risk premium, because it has no apparent correlations with typical market risk factors such as equity, inflation and foreign exchange. The resulting diversification effect allows capital market investors to expand their efficient frontiers, achieving better risk and reward combinations.

Capital market investors demand liquidity and transparency. Therefore, to attract their participation in longevity risk transfers, there is a need to package longevity risk as standardized products that are structured like typical capital market derivatives such as swaps and forwards. Hedgers have to compromise, as standardized hedging instruments do not give a full elimination of risk (which bespoke derisking solutions such as pension buyouts can offer). The act of standardization leads to a fundamental question: Given a collection of standardized mortality derivatives, how should a hedger optimize a longevity hedge? Over the past few years, there has been a wave of work on this research question. The contributions can be divided into two broad categories: (1) risk minimization and (2) sensitivity matching.

A risk minimization strategy is one that aims to minimize a certain risk measure that reflects the hedger's exposure to longevity risk. The most commonly used risk measure is the variance of the present values of the unexpected cash flows arising from the liability being hedged and the hedging instruments used. Examples of such strategies include those proposed by Dahl and Møller (2006), Dahl et al. (2008), Coughlan et al. (2011), Dahl et al. (2011), Ngai and Sherris (2011), Cairns et al. (2014) and Wong et al. (2014). These strategies are very well suited for hedgers with a definite hedging objective (e.g., minimizing variance). However, a solution that is optimum with respect to one objective may require compromising other objectives. That being said, when a hedger cares about the overall longevity risk profile (based on a collection of risk measures), then a risk minimization strategy may not result in the most preferred hedge portfolio.

A sensitivity matching strategy is one that equates the sensitivities of the liability being hedged and the hedging instruments used to changes in the underlying mortality. Rather than focusing on a particular objective, it aims to find a "replicating portfolio" that is a broadly similar to the liability being hedged in terms of its longevity risk exposure. Compared with risk minimization, sensitivity matching appears to be more flexible, as measures of mortality sensitivity can be applied to, in principle, all types of life-contingent liabilities (e.g., life insurance and annuities) and mortality derivatives (e.g., mortality forwards and swaps). It is also more adaptable to the formation of a liability hedging platform (Coughlan et al. 2007), in which risks other than longevity (e.g., equity and inflation) are also hedged so that a synthetic pension buyout can be created. This is because the other risks can be mitigated by matching additional sensitivity measures (e.g., the equity delta), without the need to re-derive the optimal solution.

Depending on how sensitivity is quantified, sensitivity-matching strategies can be further classified into two types. The first type is based on the sensitivity to the changes in the (future) mortality rates themselves. For instance, the key q-duration proposed by Li and Luo (2012) measures the sensitivity to changes in several representative mortality rates on the relevant mortality curve/surface. Other examples include those considered by Li and Hardy (2011), Plat (2011), Tsai et al. (2010), Tsai and Jiang (2011), Lin and Tsai (2013) and Tsai and Chung (2013). In addition to calibrating standardized longevity hedges, sensitivity-matching techniques have also been used in the context of natural hedging, whereby the offsetting longevity exposures in life insurance and life annuity books are utilized (see, e.g., Wang et al. 2010; Lin and Tsai 2014).

The second type, which is the focus of this paper, is based on the sensitivity to changes in certain parameter(s) in the stochastic process driving the evolution of mortality. Such measures of sensitivity are sometimes known as "longevity Greeks," as they are largely analogous to option Greeks that are utilized extensively to hedge equity-related risks. In a continuous-time setting, Luciano et al. (2012), Luciano and Regis (2014) and Luciano et al. (2015) use two longevity Greeks (delta and gamma) to develop their hedge portfolios. Their contributions have been extended by Rosa et al. (2016), who incorporate an additional longevity Greek (theta) to measure the change in the value of a life-contingent liability with respect to the passage of time. In a discrete-time setting, delta hedging has been considered by Cairns (2011) and Zhou and Li (2016), and extended by Cairns (2013) to delta-nuga hedging, which incorporates additionally the sensitivity to the drift vector of the random walk embedded in the author's assumed stochastic mortality model.

The continuous-time setting has many mathematical appeals, including analytical solutions that require no simulation to evaluate. However, it often relies on rather restrictive mortality processes, which inevitably compromise its applicability in practice. As an example, the result of Luciano et al. (2012) is developed from an Ornstein-Uhlenbeck process which captures the mortality intensity of one birth cohort only, and hence it does not facilitate the comparison between hedging instruments that are associated with different years of birth. In this paper, we choose to consider the discrete-time setting, which is more practical at the expense of more computationally involved calculations. We work along the lines of Cairns (2011) with an objective to develop a better understanding of (discrete-time) longevity Greek hedging. As described in the following paragraphs, our contributions are fourfold.

First, we propose to use two additional longevity Greeks: gamma and vega. Considered previously in the continuous-time setting, longevity gamma measures the second-order sensitivity to changes in the period (time-related) effect in the assumed mortality model, complementing the corresponding first-order sensitivity captured by longevity delta. Longevity vega, in contrast, quantifies the sensitivity to changes in the volatility of the period effects. Although longevity vega was not considered in previous studies, we believe that it is important to consider, as there exists profound evidence that the evolution of mortality over time is subject to (stochastically) varying volatility (see, e.g., Lee and Miller 2001; Gao and Hu 2009; Chai et al. 2013). In the context of equity risk, the importance of vega in a stochastic volatility environment is highlighted by Engle and Rosenberg (1995, 2000), Lehar et al. (2002), Javaheri et al. (2004) and Crépey (2004). Several researchers, including Gao and Hu (2009), Giacometti et al. (2012), Chai et al. (2013), Chen et al. (2015) and Wang and Li (2016), have used different variants of the generalized autoregressive conditional heteroskedasticity (GARCH) model to capture the stochastic volatility of mortality over time. However, they have made no attempt to relate their GARCH models to longevity hedging.

The longevity Greeks are derived from the Lee-Carter model (Lee and Carter 1992), which is augmented to incorporate stochastic volatility. In particular, the evolution of its period effect is modeled by a random walk (with drift), of which the innovations are assumed to follow a GARCH(1, 1) process. We focus on static hedges, so all longevity Greeks are calculated at time 0 when the hedge is established. The longevity vega of a liability/instrument is defined as the first derivative of its value with respect to the conditional volatility of the innovations at time 0. Likewise, longevity delta and gamma are calculated as the first and second derivatives with respect to the time-0 value of the period effect, respectively. Compared with those of Cairns (2011), our longevity Greeks are different in that they are expressed in a semi-analytical form. For this reason, the computation of our longevity Greeks does not require finite inferencing and is therefore somewhat less computationally intensive.

Second, we derive and explain the properties of the three longevity Greeks for q-forwards with different specifications. Simply speaking, a q-forward is a zero-coupon swap with its floating leg proportional to the realized death rate at a certain age (the reference age) in a certain year (the reference year) and its fixed leg proportional to the corresponding predetermined forward mortality rate. We focus on q-forwards, in part because they form basic building blocks from which other more complex mortality derivatives can be constructed (Coughlan 2009), and in part because they have been considered extensively in the literature (e.g., Cairns 2011, 2013; Cairns et al. 2014; Li and Hardy 2011; Li and Luo 2012). We found and explained that, for example, other things equal, the magnitude of the longevity gamma of a q-forward increases with its reference age. As with what have been developed for equity options (see, e.g., McDonald 2012), these properties allow us to know more about q-forwards as a risk mitigation tool. Also, in practice, when a perfect Greek neutralization is not always possible, these properties can guide the hedger to choose an appropriate q-forward that can offset his or her longevity risk exposure in a particular dimension. For instance, if the hedger has an annuity liability with a large longevity gamma, then based on our results, he or she should contemplate acquiring a q-forward with a high reference age.

Third, using the properties of longevity Greeks, we identify and explain several relationships between hedge effectiveness and q-forward specification. The results reveal several interesting facts. For example, in a delta-vega hedge formed by q-forwards, the choice of reference ages does not materially affect hedge effectiveness, but the choice of times to maturity does. What we found may aid insurers to better formulate their hedge portfolios, in terms of choosing what q-forwards to use and what longevity Greek(s) to match. The relationships we identified also allow us to go beyond the classical problem of longevity hedge optimization, shedding light on questions like "What q-forward specification is likely to be the most useful to typical hedgers?" The answers to such questions may help issuers of mortality derivatives determine what security specifications are more likely to attract demand and hence liquidity.

Fourth and finally, we investigate how much hedge effectiveness may be eroded if the mortality model from which the longevity Greeks are derived does not hold. We also examine if the identified patterns of hedge effectiveness relative to q-forward specifications are still preserved if the evolution of mortality does not follow the assumed model. To this end, we employ the nonparametric bootstrapping method considered by Li and Ng (2011), in which scenarios of future mortality are simulated by drawing pseudo samples of mortality improvement rates from the historical data. This bootstrapping method is chosen for our analyses because, among all available mortality bootstrapping methods (Brouhns et al. 2005; Koissi et al. 2006; Renshaw and Haberman 2008; Liu and Braun 2010; Li 2014; Yang et al. 2015), it appears to be the only one that entails no assumed model. So far as we aware, this study represents the first attempt to validate longevity hedging results with a nonparametric, model-free approach.

The rest of this paper is organized as follows. Section 2 introduces the extension of the Lee-Carter model that incorporates stochastic volatility. Section 3 defines the three longevity Greeks considered and derives these Greeks for annuity liabilities and q-forwards. Section 4 studies the properties of the three longevity Greeks for q-forwards with different specifications. Section 5 considers several longevity Greek hedging strategies and estimate the levels of hedge effectiveness that these strategies can possibly achieve. Section 6 validates the results in the previous section, using the nonparametric bootstrapping method. Finally, Section 7 concludes with a discussion of the limitations of this study.

2 The Lee-Carter Model With Stochastic Volatility

The model we consider is developed from the Lee-Carter structure, which assumes that

$$\ln(m_{x,t}) = \alpha_x + \beta_x \kappa_t, \tag{1}$$

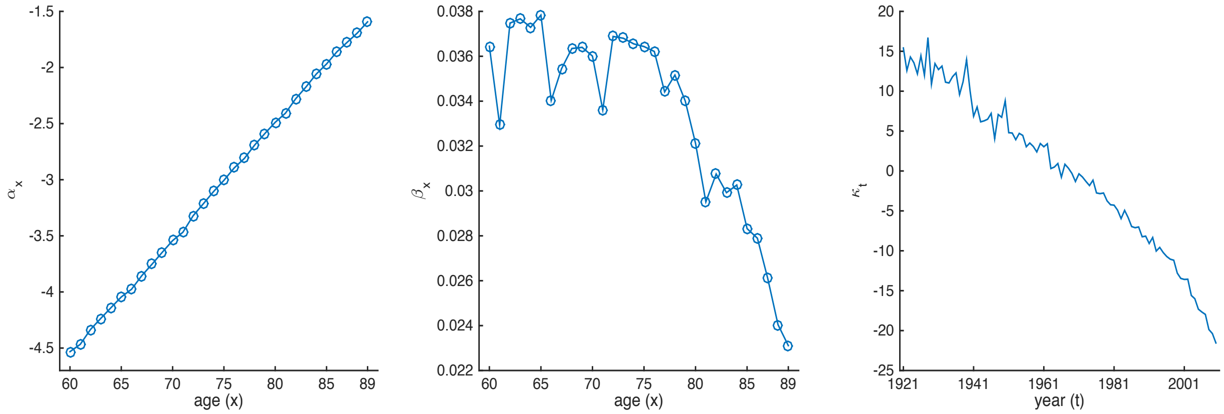

Fig. 1. Estimated Values of α_x, β_x and κ_t

where $m_{x,t}$ represents the *underlying* central death rate at age x and in year t, α_x is a parameter capturing the average level of mortality at age x, κ_t is a time-varying index (the period effect) reflecting the overall level of mortality in year t, and β_x is a parameter measuring the sensitivity of the mortality at age x to changes in κ_t.

As in many studies of the Lee-Carter model, including the original work of Lee and Carter (1992), we assume that κ_t follows a random walk with drift. However, to capture the potential stochastic volatility of mortality, we permit the innovations of the random walk to follow a GARCH(1, 1) process. Overall, the dynamics of κ_t are governed by the following set of equations:

$$\left\{ \begin{array}{rcl} \kappa_t & = & \kappa_{t-1} + \theta + \epsilon_t \\ \epsilon_t & = & \sqrt{h_t}\eta_t \\ h_t & = & \omega + a\epsilon_{t-1}^2 + bh_{t-1} \end{array} \right. , \tag{2}$$

where θ is the drift term representing the expected rate of change in κ_t, ϵ_t is the innovation at time t, h_t is the conditional variance of ϵ_t, η_t is a standard normal random variable that possesses no serial correlation, and ω, a, b are parameters in the GARCH process that determine the evolution of h_t. Parameters a and b, which respectively measure the dependence of h_t on ϵ_{t-1}^2 and h_{t-1}, play the most crucial role in modeling stochastic volatility. In the extreme case when $a = b = 0$, the volatility of ϵ_t becomes constant over time, and equation (2) degenerates to an ordinary random walk with drift.

We illustrate the proposed model using data from the female population of England and Wales (EW), over an age range of 60 to 89 and a sample period of 1921 to 2011. This data set and the estimated model are used throughout the rest of this paper.

We first use Poisson maximum likelihood (Brouhns et al. 2002) to estimate the parameters in Equation (1). The estimated values of α_x, β_x and κ_t are shown in Figure 1. Of particular interest is the pattern of κ_t. As expected, κ_t possesses a downward trend, which reflects the historical improvement in mortality. The augmented Dickey-Fuller test confirms that this trend is removed after first differencing; that is, the series of $\kappa_t - \kappa_{t-1}$ is stationary. More importantly, we observe signs of varying volatility from the pattern of κ_t, particularly during 1921–1961.

We use Engle's ARCH test and the Ljung-Box test to verify the existence of conditional heteroskedasticity. Reported in Table 1, the test results reject the null hypothesis that $(\kappa_t - \kappa_{t-1})^2$ possesses no serial correlation, confirming the existence of conditional heteroskedasticity. The test results are echoed in the sample autocorrelation function for $(\kappa_t - \kappa_{t-1})^2$ (Figure 2, left panel), from which we observe that the sample autocorrelation for $(\kappa_t - \kappa_{t-1})^2$ at lags 1, 10, 11 and 12 are significant. There is hence a strong ground for using a GARCH process for ϵ_t instead of assuming a constant volatility.

We then fit Equation (2) to the estimates of κ_t over the sample period. The retrieved values of h_t are displayed in Figure 3, while the estimates of θ, ω, a and b are reported in Table 2. The existence of conditional heteroskedasticity is further supported by the empirical facts that h_t is not constant over time

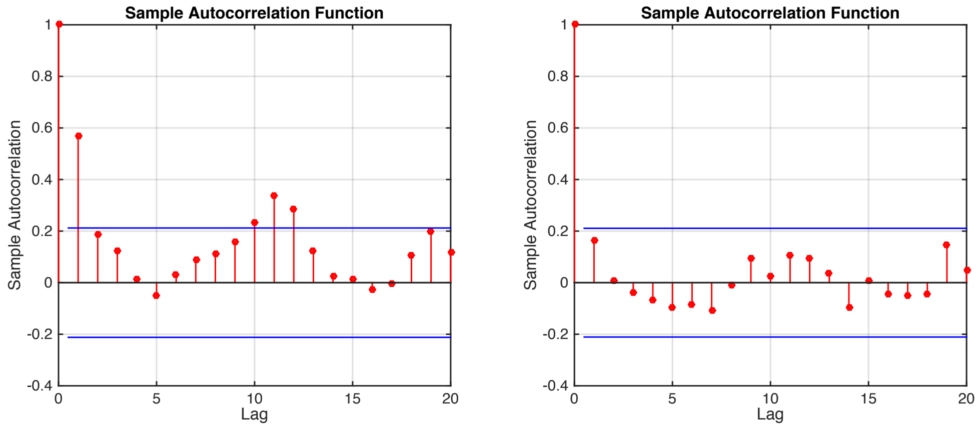

Fig. 2. Sample Autocorrelation Functions for $(\kappa_t - \kappa_{t-1})^2$ (Left Panel) and the Squared Standardized Residuals (ϵ_t^2/h_t) in Equation (2) (Right Panel), Lags 1–20

Table 1. Values of the Test Statistic for Engle's ARCH Test and the Ljung-Box Test on $(\kappa_t - \kappa_{t-1})^2$, Lags 1–5

Lag	**1**	**2**	**3**	**4**	**5**
Engle's ARCH test	19.9426 (<0.0001)	21.7042 (<0.0001)	22.8088 (<0.0001)	22.7850 (0.0001)	23.1499 (0.0003)
Ljung-Box test	20.5841 (<0.0001)	21.5166 (<0.0001)	22.2887 (<0.0001)	22.5414 (0.0002)	23.0843 (0.0003)

Note: The p-values are reported in parentheses.

and that the estimates of a and b are significantly different from 0.

Finally, we evaluate the adequacy of the assumed stochastic process by applying Engle's ARCH test and the Ljung-Box test to the squared standardized residuals (ϵ_t^2/h_t). For both tests, the null hypothesis that ϵ_t^2/h_t is free of serial correlation is not rejected (see Table 3), suggesting that conditional heteroskedasticity is adequately captured by the assumed stochastic process. The same conclusion can be drawn from the right panel of Figure 2, where we plot the sample autocorrelation function for the squared standardized residuals.

We conclude this section with two remarks. First, admittedly, the existence of conditional heteroskedasticity is data dependent. Nevertheless, it has been detected in the historical mortality experiences of quite a few other populations; see Gao and Hu (2009) for Iceland, Giacometti et al. (2012) for Italy, Chai et al. (2013) for the United Kingdom (including the part of the United Kingdom outside England and Wales), and Chen et al. (2015) and Wang and Li (2016) for Canada, France, Germany, Japan and the United States. Second, to keep the mathematics in the derivation of longevity Greeks modest, we consider only the simplest possible GARCH process and do not impose an autoregressive moving average (ARMA) structure for the conditional mean of $\kappa_t - \kappa_{t-1}$. In principle, a more general GARCH($P \geq 1$, $Q \geq 1$) process can be assumed, but as Tsay (2005, Ch.3) mentioned, in most applications only lower-order GARCH processes such as GARCH(1, 1) are used.

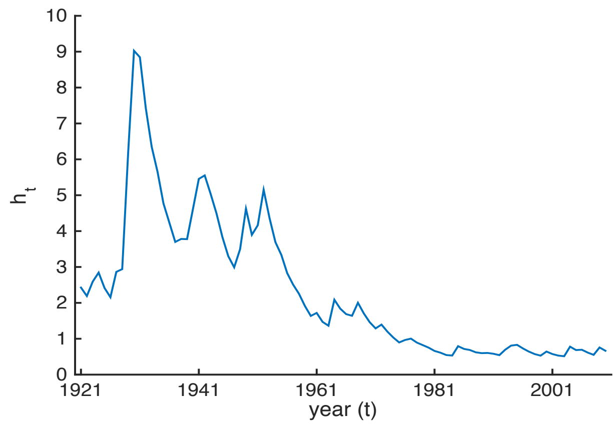

Fig. 3. Retrieved Values h_t Over the Sample Period of 1921–2011

Table 2. Estimates of θ, ω, a and b in Equation (2)

Parameter	Estimate	Standard Error	t-Value
θ	-0.49476	0.109296	-4.52677
ω	0.03297	0.046127	0.71482
a	0.13450	0.062155	2.16393
b	0.83494	0.071398	11.6941

3 The Longevity Greeks

3.1 Defining Survival Probabilities

Let

$$S_{x,t}(T) = \prod_{s=1}^{T}(1 - q_{x+s-1,t+s})$$

be the ex post probability that an individual aged x at time t would have survived to time $t+T$, where $q_{x,t}$ represents the probability that an individual aged x at time $t-1$ dies between time $t-1$ and t (during year t). Using the approximation that $q_{x,t} \approx 1 - e^{-m_{x,t}}$, which holds exact if the force of mortality between two integer ages is constant, we can express $S_{x,t}(T)$ in terms of the Lee-Carter parameters as

$$\begin{aligned} S_{x,t}(T) &\approx e^{-\sum_{s=1}^{T} e^{\alpha_{x+s-1}+\beta_{x+s-1}\kappa_{t+s}}} \\ &= e^{-\sum_{s=1}^{T} e^{Y_{x,t}(s)}} \\ &= e^{-W_{x,t}(T)}, \end{aligned}$$

where $Y_{x,t}(s) = \alpha_{x+s-1} + \beta_{x+s-1}\kappa_{t+s}$ and $W_{x,t}(T) = \sum_{s=1}^{T} e^{Y_{x,t}(s)}$ are defined for simplicity.

For ease of exposition, from now on, time $t = 0$ represents the time at which the (static) longevity hedge is established. In the illustrations, we set time 0 to the end of 2011, the year in which the data sample ends. We let $\mathcal{F}_t$ be the information about mortality up to and including time t. It is clear that for $t \geq 0$, $S_{x,t}(T)|\mathcal{F}_0$ is a random variable that depends on the random realizations of κ_s for $s = t+1, \ldots, t+T$.

According to Equation (2), we have the following expression for κ_t given $\mathcal{F}_0$:

$$\kappa_t = \kappa_0 + t\theta + \sum_{s=1}^{t} \epsilon_s = \kappa_0 + t\theta + \sum_{s=1}^{t} \sqrt{h_s}\eta_s,$$

Table 3. Values of the Test Statistic for Engle's ARCH Test and the Ljung-Box Test on the Squared Standardized Residuals (ϵ_t^2/h_t) in Equation (2), Lags 1–5

Lag	**1**	**2**	**3**	**4**	**5**
Engle's ARCH test	2.3773 (0.1231)	2.5549 (0.2787)	2.5148 (0.4726)	2.8920 (0.5761)	3.2689 (0.6586)
Ljung-Box test	2.4791 (0.1154)	2.4819 (0.2891)	2.6298 (0.4523)	3.0612 (0.5476)	3.9322 (0.5592)

Note: The p-values are reported in parentheses.

where

$$h_t = \begin{cases} \omega\left(1+\sum_{s=1}^{t-1}\prod_{u=1}^{s}(a\eta_{t-u}^2+b)\right)+(a\epsilon_0^2+bh_0)\prod_{u=1}^{t-1}(a\eta_{t-u}^2+b) & \text{if } t\geq 2 \\ \omega+a\epsilon_0^2+bh_0 & \text{if } t=1 \end{cases}.$$

It follows that $S_{x,t}(T)$ depends on κ_0 (the time-0 value of the period effect), h_0 (the time-0 value of the conditional volatility) and the sequence of i.i.d. standard normal random variables $\{\eta_s; s=1,\dots,t+T\}$.

Finally, we let

$$p_{x,t}(T,\kappa_0,h_0) := \mathrm{E}[S_{x,t}(T)\mid\mathcal{F}_0],$$

which represents the expected probability that an individual aged x at time t survives to time $t+T$, given the information about mortality up to and including time 0. Revealed later in this section, $p_{x,t}(T,\kappa_0,h_0)$ is the key building block for the expected present values of the liability being hedged and the hedging instruments at the time when the hedge is established. We can compute $p_{x,t}(T,\kappa_0,h_0)$ by simulations. Specifically, we can simulate a large number, say N, of sample paths of $\{\eta_s; s=1,\dots,t+T\}$, from which N realizations of $S_{x,t}(T)|\mathcal{F}_0$ can be obtained; the value of $p_{x,t}(T,\kappa_0,h_0)$ can be evaluated by averaging the N realizations of $S_{x,t}(T)|\mathcal{F}_0$.

3.2 The Longevity Greeks for $p_{x,t}(T,\kappa_0,h_0)$

In this section, we define the three longevity Greeks for $p_{x,t}(T,\kappa_0,h_0)$. The full derivation of each Greek is presented in Appendix A.

The longevity delta for $p_{x,t}(T,\kappa_0,h_0)$ is defined as

$$\Delta_{x,t}(T) := \frac{\partial p_{x,t}(T,\kappa_0,h_0)}{\partial\kappa_0} = -\sum_{s=1}^{T}\beta_{x+s-1}\,\mathrm{E}\left[e^{Y_{x,t}(s)-W_{x,t}(T)}\;\middle|\;\mathcal{F}_0\right], \tag{3}$$

which measures the first-order sensitivity of $p_{x,t}(T,\kappa_0,h_0)$ to κ_0 (the time-0 value of the period effect). For most mortality data sets (including the one we consider), the estimates of β_x are all positive. In this case, according to the above formula, $\Delta_{x,t}(T)$ is always negative, which means that $p_{x,t}(T,\kappa_0,h_0)$ is negatively related to κ_0.

The longevity gamma for $p_{x,t}(T,\kappa_0,h_0)$ is defined as

$$\begin{aligned}\Gamma_{x,t}(T) &:= \frac{\partial^2 p_{x,t}(T,\kappa_0,h_0)}{\partial\kappa_0^2} \\ &= \mathrm{E}\left[e^{-W_{x,t}(T)}\left(\left(\sum_{s=1}^{T}\beta_{x+s-1}e^{Y_{x,t}(s)}\right)^2-\sum_{s=1}^{T}\beta_{x+s-1}^2e^{Y_{x,t}(s)}\right)\;\middle|\;\mathcal{F}_0\right],\end{aligned} \tag{4}$$

which represents the second-order sensitivity of $p_{x,t}(T,\kappa_0,h_0)$ to κ_0 and, equivalently, the first-order sensitivity of the longevity delta $\Delta_{x,t}(T)$ to κ_0. If $\Gamma_{x,t}(T)$ is negative, then $p_{x,t}(T,\kappa_0,h_0)$ is a concave function of κ_0. The implications of the sign of $\Gamma_{x,t}(T)$ are further discussed later in Section 4.

The longevity vega for $p_{x,t}(T,\kappa_0,h_0)$ is defined as

$$
\begin{aligned}
V_{x,t}(T) &:= \frac{\partial p_{x,t}(T,\kappa_0,h_0)}{\partial h_0} \\
&= -\sum_{s=1}^{T}\beta_{x+s-1}\,\mathrm{E}\left[e^{Y_{x,t}(s)-W_{x,t}(T)}\left(\frac{\partial \kappa_{t+s}}{\partial h_0}\right)\,\middle|\,\mathcal{F}_0\right],
\end{aligned}
\tag{5}
$$

where

$$
\frac{\partial \kappa_{t+s}}{\partial h_0} = \sum_{u=1}^{t+s}\frac{\eta_u}{2\sqrt{h_u}}\frac{\partial h_u}{\partial h_0}
$$

and

$$
\frac{\partial h_u}{\partial h_0} = \begin{cases} b\prod_{v=1}^{u-1}(a\eta_{u-v}^2+b) & \text{if } u \geq 2 \\ b & \text{if } u = 1 \end{cases}.
$$

It measures the first-order sensitivity of $p_{x,t}(T,\kappa_0,h_0)$ to changes in h_0 (the time-0 value of the conditional volatility). Compared with $\Delta_{x,t}(T)$, $V_{x,t}(T)$ contains additionally $\partial\kappa_{t+s}/\partial h_0$, which measures the sensitivity of the period effect at time $t+s$ to h_0. It is also noteworthy that the longevity vega depends critically on parameter b, which measures the extent of GARCH effect (i.e., the serial dependence in the conditional variance). If b equals 0, then the longevity vega is always 0, which means that $p_{x,t}(T,\kappa_0,h_0)$ is no longer sensitive to the time-0 value of the conditional volatility.

The value of $\Delta_{x,t}(T)$, $\Gamma_{x,t}(T)$ and $V_{x,t}(T)$ can be obtained numerically. In particular, using N simulated paths of $\{\eta_s; s=1,\ldots,t+T\}$, which can be the same as those used for calculating $p_{x,t}(T,\kappa_0,h_0)$, we can readily obtain N realizations of $Y_{x,t}(s)|\mathcal{F}_0$ and $W_{x,t}(T)|\mathcal{F}_0$, with which the expectations in expressions (3), (4) and (5) can be evaluated.

3.3 The Longevity Greeks of a Stylized Pension Plan

We consider a pension plan for a single cohort of pensioners, who are aged x_0 at time 0. The plan pays each pensioner \$1 at the end of each year until death or time τ, whichever is the earliest. Let r be the constant interest rate at which future cash flows are discounted. When viewed at time 0, the present value of the pension plan's future cash flows is

$$
\mathcal{L}(x_0,\tau) = \sum_{s=1}^{\tau}(1+r)^{-s}S_{x_0,0}(s),
$$

which is a random variable that depends on the random realizations of κ_t for $t=1,\ldots,\tau$.

At time 0, the expected present value of the pension plan's future cash flows is given by

$$
L(x_0,\tau) = \mathrm{E}[\mathcal{L}\mid\mathcal{F}_0] = \sum_{s=1}^{\tau}(1+r)^{-s}p_{x_0,0}(s,\kappa_0,h_0),
$$

which is just a linear combination of various expected survival probabilities. It follows that the longevity delta, gamma and vega for the pension plan are

$$
\Delta^{(L)}(x_0,\tau) = \sum_{s=1}^{\tau}(1+r)^{-s}\Delta_{x_0,0}(s),
$$

$$
\Gamma^{(L)}(x_0,\tau) = \sum_{s=1}^{\tau}(1+r)^{-s}\Gamma_{x_0,0}(s)
$$

and

$$
V^{(L)}(x_0,\tau) = \sum_{s=1}^{\tau}(1+r)^{-s}V_{x_0,0}(s),
$$

respectively. These longevity Greeks respectively measure the first-order sensitivity of $L(x_0,\tau)$ to κ_0, the second-order sensitivity of $L(x_0,\tau)$ to κ_0, and the first-order sensitivity of $L(x_0,\tau)$ to h_0.

3.4 The Longevity Greeks of q-Forwards

A q-forward is characterized by three parameters: the reference age x^f, the time to maturity (also known as the reference year) t^f, and the forward mortality rate q^f. For a q-forward issued at time 0, the payoff to the fixed-rate receiver, payable at time t_f, is $q^f - q_{x^f,t^f}$ per \$1 notional. At an interest rate of r, its (random) discounted value at time 0 is given by

$$\begin{aligned}\mathcal{Q}(x^f, t^f) &= (1+r)^{-t^f}(q^f - q_{x^f,t^f}) \\ &= (1+r)^{-t^f}(q^f - (1 - S_{x^f,t^f-1}(1))) \\ &= (1+r)^{-t^f}(S_{x^f,t^f-1}(1) - (1-q^f)).\end{aligned}$$

Hence, at time 0, the expected present value of the q-forward's payoff from the perspective of the fixed-rate receiver is

$$Q(x^f, t^f) = \mathrm{E}[\mathcal{Q} \mid \mathcal{F}_0] = (1+r)^{-t^f}(p_{x^f,t^f-1}(1, \kappa_0, h_0) - (1-q^f)) \tag{6}$$

per \$1 notional. As $Q(x^f, t^f)$ is linearly related to $p_{x^f,t^f-1}(1, \kappa_0, h_0)$, we can easily calculate the longevity Greeks of the q-forward using what we have developed in Section 3.2. It turns out that the longevity delta, gamma and vega of the q-forward (per \$1 notional and from the fixed receiver's perspective) are

$$\Delta^{(Q)}(x^f, t^f) = (1+r)^{-t^f}\Delta_{x^f,t^f-1}(1),$$

$$\Gamma^{(Q)}(x^f, t^f) = (1+r)^{-t^f}\Gamma_{x^f,t^f-1}(1),$$

and

$$V^{(Q)}(x^f, t^f) = (1+r)^{-t^f}V_{x^f,t^f-1}(1),$$

respectively. These longevity Greeks respectively represent the first-order sensitivity of $Q(x^f, t^f)$ to κ_0, the second-order sensitivity of $Q(x^f, t^f)$ to κ_0, and the first-order sensitivity of $Q(x^f, t^f)$ to h_0. Of course, they are functions of the reference age x^f and time to maturity t^f. However, they do not depend on the forward mortality rate q^f, which appears in $Q(x^f, t^f)$ as a constant term and thus becomes irrelevant when derivative is taken.

4 Analyzing the Longevity Greeks of q-Forwards

In this section, we study the properties of the three longevity Greeks of q-forwards. All empirical illustrations are based on the data and model described in Section 2 and a constant interest rate of $r = 5\%$ per annum.

4.1 Introducing the Curve of $\exp(-\exp(Y_{x,t}(1)))$ against $Y_{x,t}(1)$

It follows from Equation (6) that the expected present value of the payoff to the fixed-rate receiver of a q-forward (with reference age x^f and time to maturity t^f) can be expressed as

$$\begin{aligned}Q(x^f, t^f) &= (1+r)^{-t^f}(p_{x^f,t^f-1}(1, \kappa_0, h_0) - (1-q^f)) \\ &= (1+r)^{-t^f}(\mathrm{E}\big[S_{x^f,t^f-1}(1) \bigm| \mathcal{F}_0\big] - (1-q^f)) \\ &= (1+r)^{-t^f}\left(\mathrm{E}\left[e^{-e^{Y_{x^f,t^f-1}(1)}} \,\middle|\, \mathcal{F}_0\right] - (1-q^f)\right),\end{aligned}$$

which is linearly related to $\mathrm{E}\big[\exp(-\exp(Y_{x^f,t^f-1}(1))) \bigm| \mathcal{F}_0\big]$.

It is clear that the curve of $\exp(-\exp(Y_{x,t}(1)))$ against $Y_{x,t}(1)$ is very influential to the expected present value and hence the longevity Greeks of a q-forward. It can be verified easily that the curve possesses the following properties:

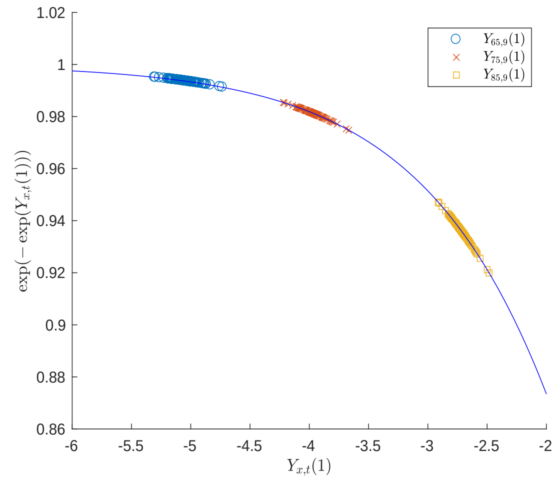

Fig. 4. The Curve $\exp(-\exp(Y_{x,t}(1)))$ Against $Y_{x,t}(1)$, for $-6 < Y_{x,t}(1) < -2$, and 100 Simulated Values of $Y_{65,9}(1)$ (Circles), $Y_{75,9}(1)$ (Crosses) and $Y_{85,9}(1)$ (Squares)

1. For all real values of $Y_{x,t}(1)$, the curve is downward sloping.
2. For all $Y_{x,t}(1) < 0$ (equivalently speaking, for all $m_{x,t} = e^{Y_{x,t}(1)} < 1$), the curve is concave.
3. For $Y_{x,t}(1) < -1$ (equivalently speaking, for all $m_{x,t} < e^{-1} \approx 0.3679$), the curve becomes increasingly concave as $Y_{x,t}$ increases.

The value of $m_{x,t}$ is typically less than the threshold of 0.3679, except for very high ages. For instance, this threshold is not exceeded until age 97 (100) for English and Welsh males (females) in 2011. In practice, it is unlikely that a q-forward with such an extremely high reference age will be available in the market. Therefore, the portion of the curve of $\exp(-\exp(Y_{x,t}(1)))$ that is of interest to us is concave, with a concavity that increases with $Y_{x,t}(1)$. Figure 4 shows the curve of $\exp(-\exp(Y_{x,t}(1)))$ for $-6 < Y_{x,t}(1) < -2$, a range that encompasses all values of $Y_{x,t}(1)|\mathcal{F}_0$ for $x = 60, \ldots, 89$ and $t = 1, \ldots, 30$, calculated from 10,000 simulated sample paths of $\{\kappa_t|\mathcal{F}_0; t = 1, \ldots, 30\}$.

Also shown in Figure 4 are 100 simulated values of $Y_{x,9}(1)|\mathcal{F}_0$, for $x = 65, 75, 85$. As x increases, the cloud of simulated values moves to the right. This outcome is not surprising, because $Y_{x,t}$, which represents the log central death rate at age x in year t, should be monotonically increasing with x when t is fixed. Consequently, for a given t, the simulated values of $Y_{x,t}(1)|\mathcal{F}_0 = (\alpha_x + \beta_x\kappa_{t+1})|\mathcal{F}_0$ tend to be larger as x increases. Similarly, because of the downward trend in κ_t, we can deduce that for a given x, the simulated values of $Y_{x,t}(1)|\mathcal{F}_0$ tend to be smaller as t increases.

The following analyses draw heavily from the facts concerning the curve of $\exp(-\exp(Y_{x,t}(1)))$ against $Y_{x,t}(1)$ and the simulated values of $Y_{x,t}(1)|\mathcal{F}_0$.

4.2 Properties of the Longevity Delta

The longevity delta of a q-forward (with reference age x^f and time to maturity t^f) is defined as the first partial derivative of $Q(x^f, t^f)$ with respect to κ_0. Assuming the expectation and differential operator can

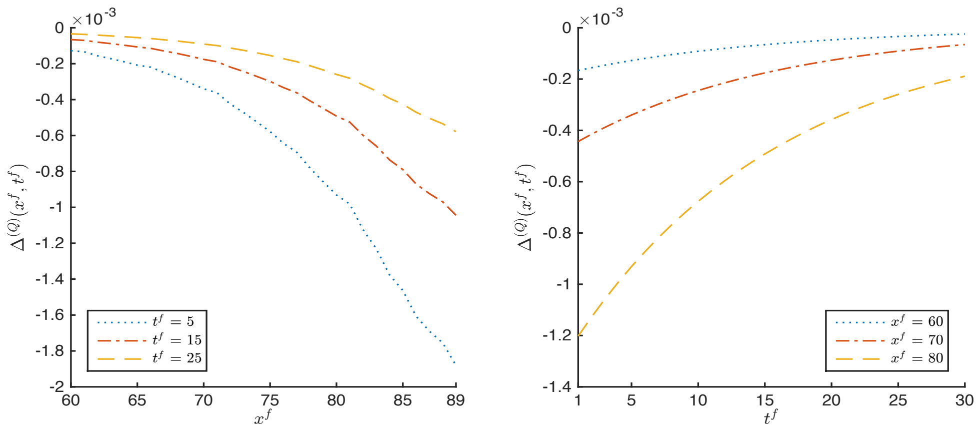

Fig. 5. The Longevity Delta of q-Forwards With Reference Ages $x^f = 60, \ldots, 89$ and Times to Maturity $1, \ldots, 30$

be interchanged, it can be expressed as

$$\begin{aligned}
\Delta^{(Q)}(x^f, t^f) &= (1+r)^{-t^f} \Delta_{x^f, t^f-1}(1) \\
&= (1+r)^{-t^f} \frac{\partial}{\partial \kappa_0} \mathrm{E}\left[e^{-e^{Y_{x^f, t^f-1}(1)}} \,\middle|\, \mathcal{F}_0 \right] \\
&= (1+r)^{-t^f} \mathrm{E}\left[\left(\frac{\partial e^{-e^{Y_{x^f, t^f-1}(1)}}}{\partial Y_{x^f, t^f-1}(1)} \right) \left(\frac{\partial Y_{x^f, t^f-1}(1)}{\partial \kappa_0} \right) \,\middle|\, \mathcal{F}_0 \right] \\
&= (1+r)^{-t^f} \beta_{x^f} \mathrm{E}\left[\frac{\partial e^{-e^{Y_{x^f, t^f-1}(1)}}}{\partial Y_{x^f, t^f-1}(1)} \,\middle|\, \mathcal{F}_0 \right]. \qquad (7)
\end{aligned}$$

Figure 5 shows the longevity deltas of q-forwards with reference ages $x^f = 60, \ldots, 89$ and times to maturity $t^f = 1, \ldots, 30$. All of the longevity deltas are negative, which is expected because the curve of $\exp(-\exp(Y_{x,t}(1)))$ against $Y_{x,t}(1)$ is always downward sloping (so that the expectation of the partial derivative is negative), and the values of β_x for all $x \in [60, 89]$ are positive.

We also observe that the longevity delta of a q-forward increases (becomes less negative) when its time to maturity t^f lengthens, but decreases (becomes more negative) when its reference age x^f rises. These trends can be explained by considering Equation (7), which suggests that the estimate of $\Delta^{(Q)}(x^f, t^f)$ is proportional to the *gradient* of the curve of $\exp(-\exp(Y_{x^f,t^f-1}(1)))$ against $Y_{x^f,t^f-1}(1)$ over the region of $Y_{x^f,t^f-1}(1)$ that the simulated values of $Y_{x^f,t^f-1}(1)|\mathcal{F}_0$ span.

As argued in Section 4.1, for a fixed x^f, the cloud of the simulated values of $Y_{x^f,t^f-1}(1)|\mathcal{F}_0$ tends to move leftward as t^f increases, lining up along the flatter portion of the curve of $\exp(-\exp(Y_{x^f,t^f-1}(1)))$ against $Y_{x^f,t^f-1}(1)$. Moreover, the discount factor in $\Delta^{(Q)}(x^f, t^f)$ approaches 0 as t^f increases. As such, the magnitude of the longevity delta is smaller as the time to maturity t^f becomes longer.

The relationship between $\Delta^{(Q)}(x^f, t^f)$ and x^f is more complicated. On one hand, the magnitude of the expectation in Equation (7) increases with x^f, as the cloud of the simulated values of $Y_{x^f,t^f-1}(1)|\mathcal{F}_0$ tends to move rightward when x^f increases. On the other hand, the magnitude of β_{x^f} reduces as x^f increases (see Figure 1). However, in this illustration, the former effect outweighs the latter, so the magnitude of the longevity delta becomes larger as the reference age x^f becomes greater.

4.3 Properties of the Longevity Gamma

The longevity delta of a q-forward (with reference age x^f and time to maturity t^f) is defined as the second partial derivative of $Q(x^f, t^f)$ with respect to κ_0. Assuming the expectation and differential operator are

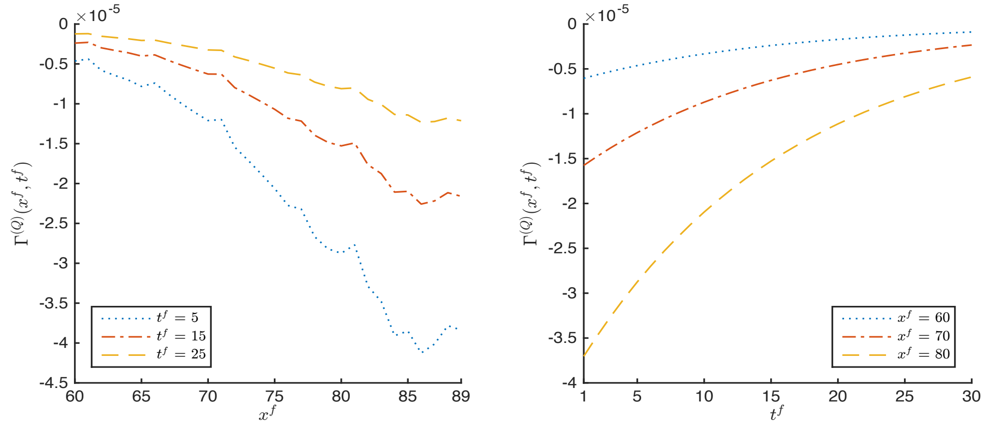

Fig. 6. The Longevity Gamma of *q*-Forwards With Reference Ages $x^f = 60, \ldots, 89$ and Times to Maturity $t^f = 1, \ldots, 30$

interchangeable, it can be expressed as

$$\begin{aligned}\Gamma^{(Q)}(x^f, t^f) &= (1+r)^{-t^f}\Gamma_{x^f,t^f-1}(1),\\ &= (1+r)^{-t^f}\frac{\partial^2}{\partial \kappa_0^2}\,\mathrm{E}\left[e^{-e^{Y_{x^f,t^f-1}(1)}}\,\middle|\,\mathcal{F}_0\right]\\ &= (1+r)^{-t^f}\beta_{x^f}^2\,\mathrm{E}\left[\frac{\partial^2 e^{-e^{Y_{x^f,t^f-1}(1)}}}{\partial(Y_{x^f,t^f-1}(1))^2}\,\middle|\,\mathcal{F}_0\right].\end{aligned} \tag{8}$$

Figure 6 shows the longevity gamma of q-forwards with reference ages $x^f = 60, \ldots, 89$ and times to maturity $t^f = 1, \ldots, 30$. The following observations can be made:

- As the curve of $\exp(-\exp(Y_{x^f,t^f-1}(1)))$ against $Y_{x^f,t^f-1}(1)$ is concave, the expectation of the second partial derivative in Equation (8) is negative, and so is $\Gamma^{(Q)}(x^f, t^f)$.
- As t^f increases, the cloud of the simulated values of $Y_{x^f,t^f-1}(1)|\mathcal{F}_0$ tends to move leftward where the curve of $\exp(-\exp(Y_{x^f,t^f-1}(1)))$ against $Y_{x^f,t^f-1}(1)$ is less concave, so the expectation of the second partial derivative in Equation (8) becomes less negative. Compounded by the fact that the discount factor diminishes with t^f, the value of $\Gamma^{(Q)}(x^f, t^f)$ becomes less negative as t^f increases.
- The relationship between $\Gamma^{(Q)}(x^f, t^f)$ and x^f depends on two offsetting effects. As x^f increases, the cloud of the simulated values of $Y_{x^f,t^f-1}(1)|\mathcal{F}_0$ tends to move rightward where the curve of $\exp(-\exp(Y_{x^f,t^f-1}(1)))$ against $Y_{x^f,t^f-1}(1)$ is more concave, which in turn means that the expectation of the second partial derivative in Equation (8) becomes larger in magnitude. On the other hand, as x^f increases, the magnitude of β_{x^f} reduces (see Figure 1). For $x^f < 85$, β_{x^f} reduces rather gently with x^f, so the former effect dominates, and the magnitude of $\Gamma^{(Q)}(x^f, t^f)$ increases with x^f. However, the opposite is true for $x^f > 85$ when β_{x^f} reduces rapidly with x^f.
- The relationship between $\Gamma^{(Q)}(x^f, t^f)$ and x^f is somewhat jagged. The jaggedness arises because the estimates of β_x are not perfectly smooth across ages (see Figure 1).

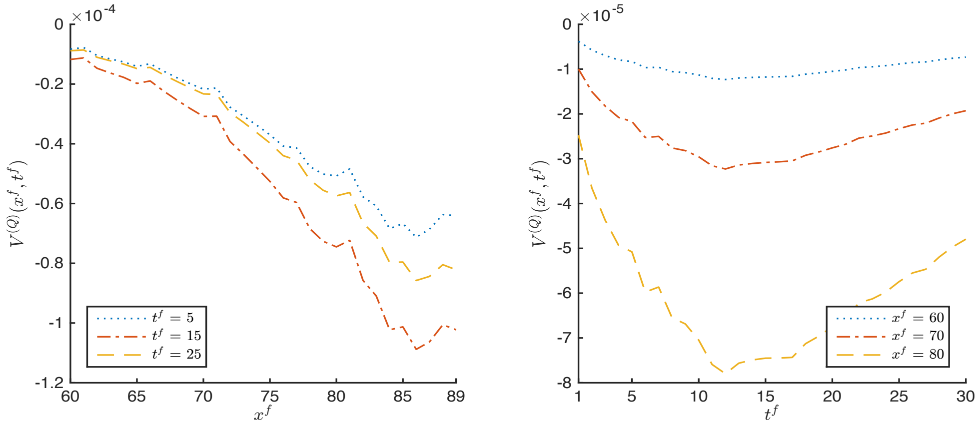

Fig. 7. The Longevity Vega of q-Forwards With Reference Ages $x^f = 60, \ldots, 89$ and Times to Maturity $1, \ldots, 30$

4.4 Properties of the Longevity Vega

In terms of $Y_{x^f,t^f-1}(1)$, the longevity vega of a q-forward (with reference age x^f and time to maturity t^f) can be expressed as

$$\begin{aligned} V^{(Q)}(x^f,t^f) &= (1+r)^{-t^f} V_{x^f,t^f-1}(1), \\ &= (1+r)^{-t^f} \frac{\partial}{\partial h_0} \mathrm{E}\left[e^{-e^{Y_{x^f,t^f-1}(1)}} \,\middle|\, \mathcal{F}_0 \right], \end{aligned} \tag{9}$$

which suggests that from a numerical perspective, $V^{(Q)}(x^f,t^f)$ measures how the average of the simulated values of $\exp(-\exp(Y_{x^f,t^f-1}(1)))$ will change when the time-0 conditional volatility h_0 increases by an arbitrarily small amount.

Figure 7 shows the longevity vega of q-forwards with reference ages $x^f = 60, \ldots, 89$ and times to maturity $t^f = 1, \ldots, 30$. As with the longevity delta and gamma, the longevity vega is negative for all reference ages and times to maturity considered. A negative longevity vega means that the expected present value of a q-forward decreases as the conditional volatility (h_0) of the current period effect increases. The negativeness of the longevity vega is related to the concavity of the curve of $\exp(-\exp(Y_{x^f,t^f-1}(1)))$ against $Y_{x^f,t^f-1}(1)$, which means that the sensitivity of $\exp(-\exp(Y_{x^f,t^f-1}(1)))$ to changes in $Y_{x^f,t^f-1}(1)$ is asymmetric. When h_0 increases, the range of the simulated values of $Y_{x^f,t^f-1}(1)|\mathcal{F}_0$ widens symmetrically around $\mathrm{E}\big[Y_{x^f,t^f-1}(1) \,\big|\, \mathcal{F}_0\big]$; however, because of the asymmetric sensitivity, the average of the simulated values of $\exp(-\exp(Y_{x^f,t^f-1}(1)))|\mathcal{F}_0$ reduces, thereby resulting in a negative longevity vega.[1] This phenomenon is demonstrated in Figure 8, which compares the simulated values of $\exp(-\exp(Y_{x,t}(1)))|\mathcal{F}_0$ that are based on two different assumed values of h_0.

The relationship between the longevity vega and the reference age (x^f) is a result of the trade-off between two offsetting effects:

1. When x^f increases, the cloud of the simulated values of $Y_{x^f,t^f-1}(1)|\mathcal{F}_0$ tends to move rightward where the curve of $\exp(-\exp(Y_{x^f,t^f-1}(1)))$ against $Y_{x^f,t^f-1}(1)$ is more concave. The effect of asymmetric sensitivity becomes more severe, thereby pushing the longevity vega more negative.

2. When x^f increases, β_{x^f} reduces, and so does the variance of $Y_{x^f,t^f-1}(1)|\mathcal{F}_0$ (which is proportional to the square of β_{x^f}). As the simulated values of $Y_{x^f,t^f-1}(1)|\mathcal{F}_0$ span a smaller range, the effect of asymmetric sensitivity becomes less significant, and hence the longevity vega tends to be less negative.

[1] According to Theorem 2 in Section 5.3, the third moment of $\kappa_{t^f}|\mathcal{F}_0$ about its mean is 0. It follows that the distribution of $Y_{x^f,t^f-1}(1) = \alpha_{x^f} + \beta_{x^f}\kappa_{t^f}$ given $\mathcal{F}_0$ is symmetric.

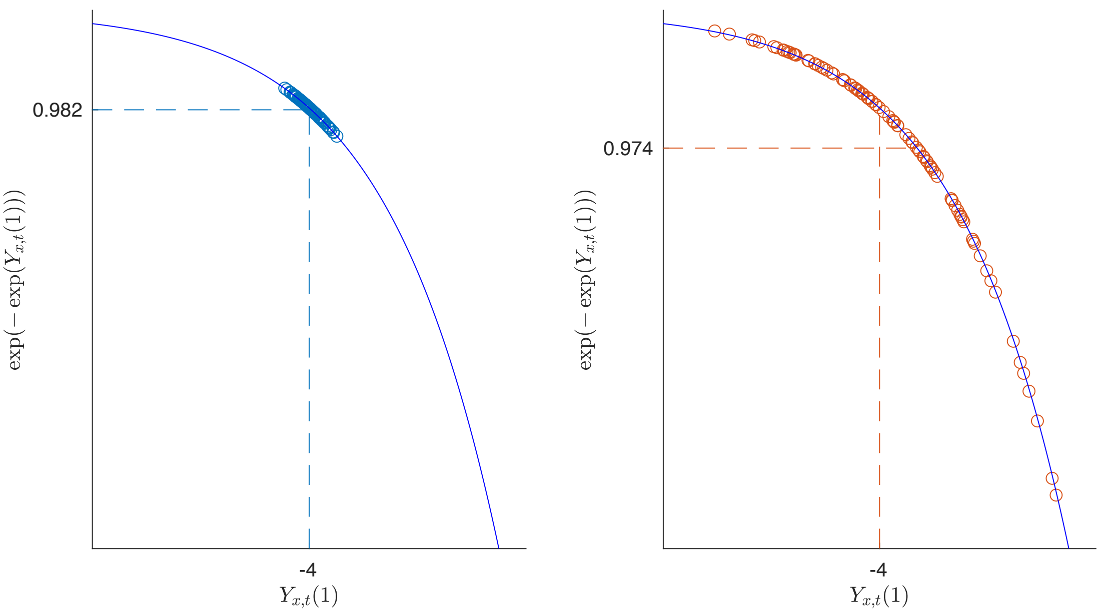

Fig. 8. Simulated Values of $\exp(-\exp(Y_{x,t}(1)))|\mathcal{F}_0$ Based on a Smaller Value of h_0 (Left Panel) and a Larger Value of h_0 (Right Panel)

Note: The values of x and t used are arbitrary.

As seen in the left panel of Figure 7, in this illustration the first effect dominates for $x^f < 85$, but the opposite happens when $x^f > 85$.

The relationship between the longevity vega and the time to maturity (t^f) depends on the following three factors:

1. Given the assumed stochastic process for κ_t, the volatility of $\kappa_{t^f}|\mathcal{F}_0$ increases with t^f. As such, when t^f increases, the volatility of $Y_{x^f,t^f-1}(1)|\mathcal{F}_0 = (\alpha_{x^f} + \beta_{x^f}\kappa_{t^f})|\mathcal{F}_0$ increases, and thus the simulated values of $Y_{x^f,t^f-1}(1)|\mathcal{F}_0$ span a wider range. Consequently, the effect of asymmetric sensitivity becomes more significant, thereby pushing the longevity vega more negative.

2. As t^f increases, the cloud of the simulated values of $Y_{x^f,t^f-1}(1)|\mathcal{F}_0$ tends to move leftward where the curve of $\exp(-\exp(Y_{x^f,t^f-1}(1)))$ against $Y_{x^f,t^f-1}(1)$ is less concave. The effect of asymmetric sensitivity becomes less significant, so the longevity vega tends to be less negative.

3. As t^f increases, the discount factor in equation (9) reduces, so the longevity vega tends to be less negative.

The first factor dominates when t^f is small, but the second and third factors become more influential when t^f is high. In this illustration, the turning point is at $t^f = 12$ (see the right panel of Figure 7).

5 Greek Hedging of Longevity Risk

In this section, we consider different static longevity Greek hedging strategies, and investigate how much hedge effectiveness can be obtained using different combinations of longevity Greeks and q-forwards.

5.1 Assumptions

The following assumptions are used in the rest of this section:

1. The liability being hedged is a pension plan for a single cohort of individuals aged $x_0 = 60$ at time 0. The pension plan pays each pensioner \$1 at the end of each year until age 89 or death, whichever is the earliest (i.e., $\tau = 30$).
2. At time 0, a static longevity hedge for the pension plan is constructed using one or two q-forwards.
3. At time 0, q-forwards with reference ages $x^f = 60, \ldots 89$ and times to maturity $t^f = 1, \ldots, 30$ years are available. The q-forwards' reference population is the England and Wales (EW) female population.
4. The mortality experience of the plan members is identical to that of the EW female population, so that there is no population basis risk.
5. The interest rate for all durations is $r = 5\%$ per annum.
6. The longevity Greeks are numerically calculated based on 10,000 mortality scenarios that are generated from the model described in Section 2.

Under these assumptions, the longevity Greeks of the liability being hedged are fixed regardless of how many q-forwards are used and what the reference age(s) and time(s) to maturity are. It turns out that the liability being hedged has an expected present value of $L(60, 30) = 13.4403$, a longevity delta $\Delta^{(L)}(60, 30) = -0.0562$, a longevity gamma of $\Gamma^{(L)}(60, 30) = -0.0014$, and a longevity vega of $V^{(L)}(60, 30) = -0.0053$.

5.2 The Evaluation Metric

We measure hedge effectiveness with the following metric:

$$\text{HE} = 1 - \frac{\text{Var}(\mathcal{L}(60, 30) - \sum_{i=1}^{\mathcal{J}} u(x_i^f, t_i^f)\mathcal{Q}(x_i^f, t_i^f)|\mathcal{F}_0)}{\text{Var}(\mathcal{L}(60, 30)|\mathcal{F}_0)}, \tag{10}$$

where

- $\mathcal{J}$ denotes the number of q-forwards used,
- $u(x_i^f, t_i^f)$ represents the notional amount of the ith q-forward used, and
- x_i^f and t_i^f are the reference age and time to maturity for the ith q-forward used, respectively.

In the fraction, the numerator is the hedged position's variance, whereas the denominator is the unhedged position's variance. It follows that a value of HE that is close to 1 indicates a good hedge effectiveness.

We simulate 10,000 mortality scenarios on top of those used for calculating the longevity Greeks. The additional 10,000 simulated mortality scenarios enable us to calculate realizations of $\mathcal{L}(60, 30)|\mathcal{F}_0$ and $\mathcal{Q}(x^f, t^f)|\mathcal{F}_0$, with which the value of HE can be estimated.

5.3 Single Longevity Greek Hedging

When using $\mathcal{J} = 1$ q-forward to match one longevity Greek, we find the required notional amount by setting

$$\mathcal{G}^{(L)}(60, 30) - u^{(\mathcal{G})}(x^f, t^f)\mathcal{G}^{(Q)}(x^f, t^f) = 0,$$

which gives

$$u^{(\mathcal{G})}(x^f, t^f) = \frac{\mathcal{G}^{(L)}(60, 30)}{\mathcal{G}^{(Q)}(x^f, t^f)},$$

where $\mathcal{G} = \Delta, V$ represents the longevity Greek being matched. We do not consider gamma hedges here, as it does not seem legitimate to match the second-order sensitivity to κ_0 without matching the first-order sensitivity.

It is clear that the notional amount and hence the hedge effectiveness depend on $\mathcal{G}$, x^f and t^f. Figure 9 (left and middle panels) shows the values of HE for $\mathcal{G} = \Delta, V$, $x^f = 60, \ldots, 89$ and $t^f = 1, \ldots, 30$.

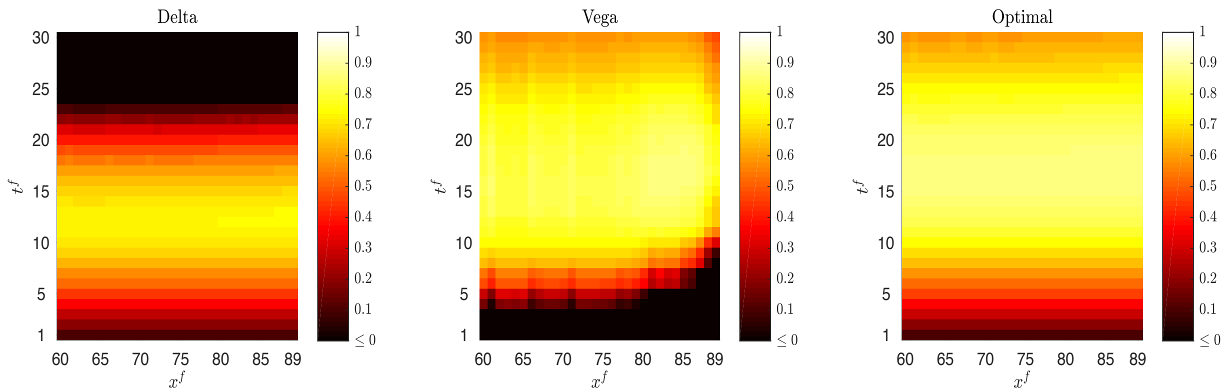

Fig. 9. Values of HE for the Delta Hedges (Left), Vega Hedges (Center) and Ex Post Optimal Hedges (Right) With $\mathcal{J} = 1$ *q*-Forward, $x^f = 60, \ldots, 89$ and $t^f = 1, \ldots, 30$

We also benchmark the Greek hedges against the corresponding ex post "optimal" hedges, which are obtained by searching for the notional amount that minimizes the hedged position's variance. Following the results of Cairns et al. (2014), for a hedge with $\mathcal{J} = 1$ q-forward, the ex post optimal notional amount is

$$u^{(\text{opt})}(x^f, t^f) = \sqrt{\frac{\text{Var}(\mathcal{L}(60,30)|\mathcal{F}_0)}{\text{Var}(\mathcal{Q}(x^f, t^f)|\mathcal{F}_0)}} \times \text{Corr}(\mathcal{L}(60,30), \mathcal{Q}(x^f, t^f)|\mathcal{F}_0), \tag{11}$$

which gives a hedge effectiveness equal to the square of $\text{Corr}(\mathcal{L}(60,30), \mathcal{Q}(x^f, t^f)|\mathcal{F}_0)$. The variances and correlation in Equation (11) are estimated using the 10,000 mortality scenarios which we use to evaluate the Greek hedges. The right panel of Figure 9 shows the ex post optimal hedge effectiveness for different combinations of x^f and t^f.

Several interesting relationships are observed in Figure 9. First, for a given time to maturity, the hedge effectiveness is insensitive to the choice of the reference age. This outcome is not overly surprising, because the assumed Lee-Carter structure implies that $\ln(m_{x,t})$ and $\ln(m_{y,t})$ are perfectly correlated even if $x \neq y$. As such, q-forwards with the same time to maturity but different reference ages should result in similar levels of hedge effectiveness.

Second, a delta hedge is almost equally effective as the ex post optimal hedge when the q-forward's time to maturity is short (less than 15 years) but is very ineffective when the q-forward's time to maturity is long. This outcome can be attributed to the pattern of $\Delta^{(Q)}(x^f, t^f)$ against t^f (Figure 5, right panel), which implies that in a delta hedge, the notional amount $u^{(\Delta)}(x^f, t^f) = \Delta^{(L)}(60, 30)/\Delta^{(Q)}(x^f, t^f)$ of the q-forward increases rapidly as t^f increases. However, the optimal notional amount $u^{(\text{opt})}(x^f, t^f)$ does not increases rapidly with t^f. In effect, as t^f increases, $u^{(\Delta)}(x^f, t^f)$ moves away from $u^{(\text{opt})}(x^f, t^f)$, leading to a highly suboptimal hedge effectiveness. See Figure 10 for an illustration.

Third, in contrast, the effectiveness of a vega hedge approaches that of the ex post optimal hedge when the q-forward's time to maturity becomes longer. This relationship is associated with the moments of κ_{t_f} (about its mean) under the assumed GARCH process. In more detail, recall that $Q(x^f, t^f)$ (the expected present value of the payoff from a q-forward with reference age x^f and time to maturity t^f) is linearly related to

$$p_{x_f, t_f - 1}(1, \kappa_0, h_0) = \text{E}\Big[e^{-e^{\alpha_{x_f} + \beta_{x_f}\kappa_{t_f}}} \;\Big|\; \mathcal{F}_0\Big] = \text{E}\big[f(\kappa_{t_f}) \;\big|\; \mathcal{F}_0\big],$$

where

$$f(\kappa_{t_f}) := e^{-e^{\alpha_{x_f} + \beta_{x_f}\kappa_{t_f}}}$$

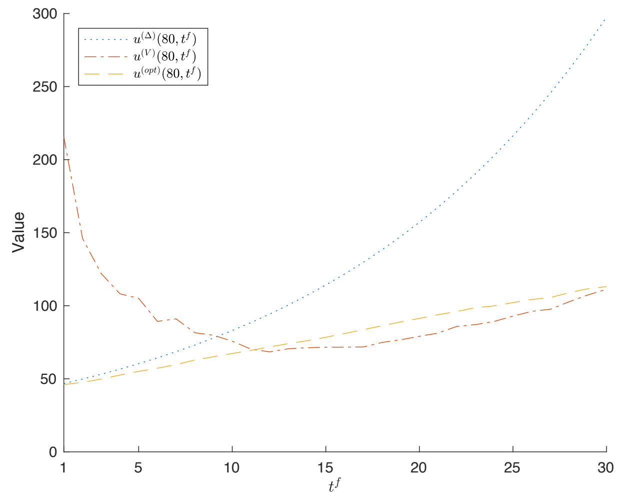

Fig. 10. Notional Amount of the Delta Hedge, Vega Hedge and Optimal Hedge That Are Built Using a *q*-Forward With Reference Age $x^f = 80$ and Times to Maturity $t^f = 1, \ldots, 30$

is defined for convenience. Using a fourth-order Taylor's expansion, we have

$$\begin{aligned} p_{x_f,t_f1}(1,\kappa_0,h_0) \approx & f(\kappa_0 + t^f\theta) + \frac{1}{2!}\frac{\partial^2 f}{\partial \kappa_{t^f}^2}\,\mathrm{E}\left[\left(\sum_{s=1}^{t_f}\sqrt{h_s}\eta_s\right)^2 \,\middle|\, \mathcal{F}_0\right] \\ & + \frac{1}{3!}\frac{\partial^3 f}{\partial \kappa_{t^f}^3}\,\mathrm{E}\left[\left(\sum_{s=1}^{t_f}\sqrt{h_s}\eta_s\right)^3 \,\middle|\, \mathcal{F}_0\right] + \frac{1}{4!}\frac{\partial^4 f}{\partial \kappa_{t^f}^4}\,\mathrm{E}\left[\left(\sum_{s=1}^{t_f}\sqrt{h_s}\eta_s\right)^4 \,\middle|\, \mathcal{F}_0\right], \end{aligned}$$

where partial derivatives are evaluated at $\mathrm{E}\big[\kappa_{t_f} \bigm| \mathcal{F}_0\big] = \kappa_0 + t^f\theta$, which is free of h_0. The moments of $\sum_{s=1}^{t_f}\sqrt{h_s}\eta_s$ (i.e., the moments of κ_{t_f} about its mean) satisfy the following results.

Theorem 1. *For $t_f \geq 1$,*

$$\mathrm{E}\left[\left(\sum_{s=1}^{t_f}\sqrt{h_s}\eta_s\right)^2 \,\middle|\, \mathcal{F}_0\right] = z_{t_f,0} + z_{t_f,1}h_0, \tag{12}$$

where $z_{t_f,0}$ and $z_{t_f,1}$ do not depend on h_0.

Proof. See Appendix B. □

Theorem 2. *For $t^f \geq 1$,*

$$\mathrm{E}\left[\left(\sum_{s=1}^{t^f}\sqrt{h_s}\eta_s\right)^3 \,\middle|\, \mathcal{F}_0\right] = 0. \tag{13}$$

Proof. See Appendix C. □

Theorem 3. *For $t^f \geq 1$,*

$$\mathrm{E}\left[\left(\sum_{s=1}^{t^f}\sqrt{h_s}\eta_s\right)^4 \,\middle|\, \mathcal{F}_0\right] = c_{t^f,0} + c_{t^f,1}h_0 + c_{t^f,2}h_0^2, \tag{14}$$

where $c_{t^f,0}$, $c_{t^f,1}$ and $c_{t^f,2}$ do not depend on h_0. Furthermore, $c_{t^f,1}$ tends to ∞ as $t^f \to \infty$, and if $3a^2 + 2ab + b^2 < 1$, then $c_{t^f,2}$ tends to a constant as $t^f \to \infty$.

Proof. See Appendix D. □

Our estimated GARCH(1, 1) model satisfies the condition that $3a^2 + 2ab + b^2 < 1$ (see Table 2).[2] It follows from the results above that $Q(x^f, t^f)$ is approximately a quadratic function of h_0, with a curvature that diminishes as t^f tends to infinity. In other words, the longevity vega $V^{(Q)}(x^f, t^f) = \partial Q(x^f, t^f)/\partial h_0$ tends to be a more accurate measure of the sensitivity of $Q(x^f, t^f)$ to h_0 as t^f increases, and thus the effectiveness of a vega hedge tends to be closer to that of the ex post optimal hedge for higher values of t^f.

5.4 Multiple Longevity Greek Hedging

5.4.1 Calculating the Notional Amounts

We now consider matching two longevity Greeks with $\mathcal{J} = 2$ q-forwards. We let $\mathcal{G}_1$ and $\mathcal{G}_2$ be the two longevity Greeks being matched, and $u^{(\mathcal{G}_1,\mathcal{G}_2)}(x_1^f, t_1^f)$ and $u^{(\mathcal{G}_1,\mathcal{G}_2)}(x_2^f, t_2^f)$ be the notional amounts of the two q-forwards in the resulting hedge portfolio. We have

$$\begin{pmatrix} \mathcal{G}_1^{(Q)}(x_1^f, t_1^f) & \mathcal{G}_1^{(Q)}(x_2^f, t_2^f) \\ \mathcal{G}_2^{(Q)}(x_1^f, t_1^f) & \mathcal{G}_2^{(Q)}(x_2^f, t_2^f) \end{pmatrix} \begin{pmatrix} u^{(\mathcal{G}_1,\mathcal{G}_2)}(x_1^f, t_1^f) \\ u^{(\mathcal{G}_1,\mathcal{G}_2)}(x_2^f, t_2^f) \end{pmatrix} = \begin{pmatrix} \mathcal{G}_1^{(L)}(60, 30) \\ \mathcal{G}_2^{(L)}(60, 30) \end{pmatrix}, \tag{15}$$

which gives

$$u^{(\mathcal{G}_1,\mathcal{G}_2)}(x_1^f, t_1^f) = \frac{\mathcal{G}_1^{(L)}(60,30)\mathcal{G}_2^{(Q)}(x_2^f, t_2^f) - \mathcal{G}_1^{(Q)}(x_2^f, t_2^f)\mathcal{G}_2^{(L)}(60,30)}{\mathcal{G}_1^{(Q)}(x_1^f, t_1^f)\mathcal{G}_2^{(Q)}(x_2^f, t_2^f) - \mathcal{G}_1^{(Q)}(x_2^f, t_2^f)\mathcal{G}_2^{(Q)}(x_1^f, t_1^f)} \tag{16}$$

and

$$u^{(\mathcal{G}_1,\mathcal{G}_2)}(x_2^f, t_2^f) = \frac{\mathcal{G}_2^{(L)}(60,30)\mathcal{G}_1^{(Q)}(x_1^f, t_1^f) - \mathcal{G}_2^{(Q)}(x_1^f, t_1^f)\mathcal{G}_1^{(L)}(60,30)}{\mathcal{G}_1^{(Q)}(x_1^f, t_1^f)\mathcal{G}_2^{(Q)}(x_2^f, t_2^f) - \mathcal{G}_1^{(Q)}(x_2^f, t_2^f)\mathcal{G}_2^{(Q)}(x_1^f, t_1^f)}. \tag{17}$$

It is clear that $u^{(\mathcal{G}_1,\mathcal{G}_2)}(x_1^f, t_1^f)$ and $u^{(\mathcal{G}_1,\mathcal{G}_2)}(x_2^f, t_2^f)$ depend on the two q-forwards' specifications as well as the two matched longevity Greeks $(\mathcal{G}_1, \mathcal{G}_2)$, which can be either (Δ, Γ) or (Δ, V). We do not consider (Γ, V), because it does not seem appropriate to match Γ without matching Δ.

A necessary (but not sufficient) condition for two q-forwards with *different* times to maturity to provide risk reduction is that the notional amounts of both q-forwards must be positive; that is, the hedger must be the fixed leg receiver in both q-forwards. This condition can explained as follows.

- When both notional amounts are negative, the present values of the q-forward portfolio and the pension liability change in the same direction for any departure from the expected mortality trajectory. The pension plan provider will be subject to even more longevity risk compared with the naked position.
- If one notional amount is negative and the other is positive, then the hedged position will be very vulnerable to "nonlinear" mortality scenarios. To illustrate, let us suppose that the notional amount of the shorter-dated q-forward is negative, while that of the longer-dated is positive. Suppose further that on the earlier maturity date, the realized mortality is lower than expected, so that the hedger suffers a loss (arising from both the unexpected increase in the pension liability and the net payment to the q-forward's counterparty). If the realized mortality on the later maturity date is also lower than expected, then the payoff from the longer-dated q-forward may defray the earlier hedge loss (provided that the notional amount of the longer-dated q-forward is sufficiently large). However, if it turns out to be higher than expected (i.e., a "nonlinear" scenario), then the earlier hedge loss can never be recovered.

We remark that this condition does not apply when the q-forwards have the same time to maturity, because in this case, the payoffs from both q-forwards are made at the same time.

[2] All stationary ARCH(1) models (in which $a = 0$ and $b < 1$) meet this condition. However, admittedly, not all GARCH(1, 1) models satisfy this condition, even if they are stationary with $a + b < 1$.

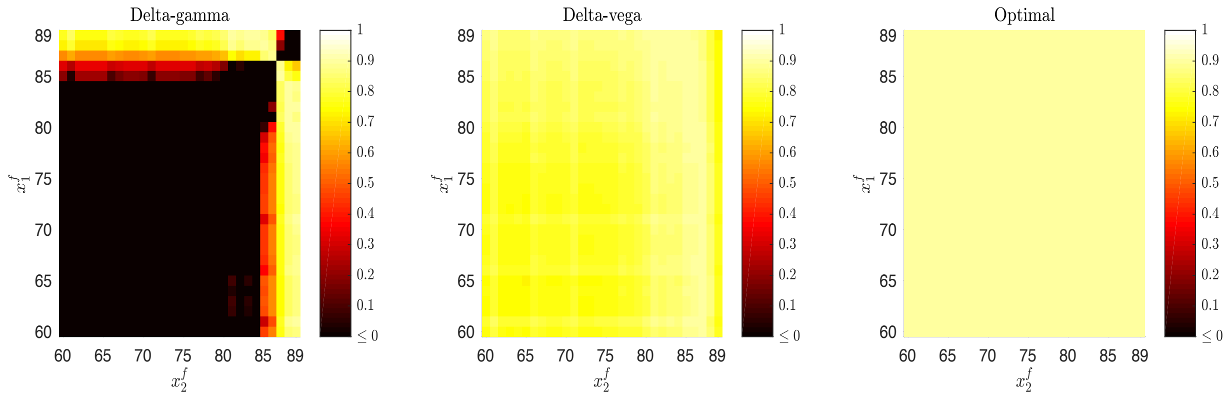

Fig. 11. Values of HE for the Delta-Gamma Hedges (Left), Delta-Vega Hedges (Center) and Ex Post Optimal Hedges (Right) With $\mathcal{J} = 2$ q-Forwards, $t_1^f = 5$, $t_2^f = 15$, $x_1^f, x_2^f = 60, \ldots, 89$

Using Equations (16) and (17), it can be shown straightforwardly that to have both $u^{(\mathcal{G}_1,\mathcal{G}_2)}(x_1^f, t_1^f)$ and $u^{(\mathcal{G}_1,\mathcal{G}_2)}(x_2^f, t_2^f)$ being positive, we require

$$\frac{\mathcal{G}_1^{(Q)}(x_1^f, t_1^f)}{\mathcal{G}_2^{(Q)}(x_1^f, t_1^f)} > \frac{\mathcal{G}_1^{(L)}(60, 30)}{\mathcal{G}_2^{(L)}(60, 30)} > \frac{\mathcal{G}_1^{(Q)}(x_2^f, t_2^f)}{\mathcal{G}_2^{(Q)}(x_2^f, t_2^f)}, \tag{18}$$

that is, the ratio of the two matched longevity Greeks for the liability being hedged must be strictly in between those of the two q-forwards. This necessary condition explains many of the hedging results we are about to present.

5.4.2 Impact of the Reference Age Combinations

We now examine the effectiveness of the delta-gamma and delta-vega hedges for different reference ages when the times to maturity are fixed to 5 and 15 years, respectively. As in the previous subsection, we benchmark the Greek hedges against their corresponding ex post optimal hedges, which are obtained by minimizing the hedged position's variance on the basis of the 10,000 mortality scenarios used for evaluating the Greek hedges. The hedging results are displayed in Figure 11. For delta-gamma hedges, most reference age combinations yield low or even negative hedge effectiveness; a meaningful reduction in risk happens only when one reference age is greater than 86 but the other is not. In contrast, for delta-vega hedges, the hedge effectiveness is much more robust relative to the choice of reference ages, and is much closer to that produced by the corresponding ex post optimal hedges.

To explain the hedging results, let us study Figure 12, which demonstrates how the delta/gamma and delta/vega ratios of a q-forward may vary with its reference age when its time to maturity is fixed. Also shown in Figure 12 are the corresponding delta/gamma and delta/vega ratios for the liability being hedged (the solid horizontal lines).

Let us first focus on the delta/gamma ratios (the left panel of Figure 12). The delta/gamma ratio of a q-forward depends quite heavily on its reference age. The sensitivity to x^f can be understood from the following formula:

$$\frac{\Delta^{(Q)}(x^f, t^f)}{\Gamma^{(Q)}(x^f, t^f)} = \frac{\mathrm{E}\left[e^{Y_{x^f,t^f-1}(1) - W_{x^f,t^f-1}(1)} \,\middle|\, \mathcal{F}_0\right]}{\beta_{x^f}\,\mathrm{E}\left[e^{Y_{x^f,t^f-1}(1) - W_{x^f,t^f-1}(1)}\left(1 - e^{Y_{x^f,t^f-1}(1)}\right) \,\middle|\, \mathcal{F}_0\right]}, \tag{19}$$

which says that the delta/gamma ratio is inversely related to β_{x^f}. Indeed, the pattern of the delta/gamma ratios against x^f is reminiscent of the pattern of β_x against x (Figure 1). However, the trends for $t^f = 5$ and $t^f = 15$ almost overlap each other, indicating that the delta/gamma ratio is very insensitive to its reference age. From the graph, it is quite clear that in order to satisfy the necessary condition specified

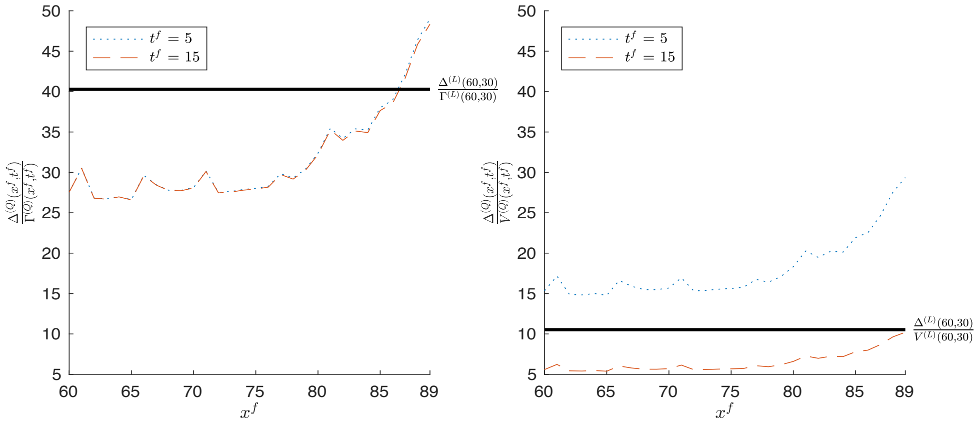

Fig. 12. Delta/Gamma (Left) and Delta/Vega (Right) Ratios for *q*-Forwards With $t^f = 5, 15$ and $x^f = 60, \ldots, 89$

Note: The solid horizontal line in the left (right) panel represents the delta/gamma (delta/vega) ratio for the liability being hedged.

by (18), one q-forward in the portfolio must have a reference age less than or equal to 86, and the other must have a reference age greater than 86.

Next, we turn to the delta/vega ratios (the right panel of Figure 12). In stark contrast, the delta/vega ratios of a q-forward are rather sensitive to its time-to-maturity (the trends for $t^f = 5$ and $t^f = 15$ are far apart) but are relatively less sensitive to its reference age. The following formula casts some light on the observed sensitivity to t^f and insensitivity to x^f:

$$\frac{\Delta^{(Q)}(x^f, t^f)}{V^{(Q)}(x^f, t^f)} = \frac{\mathrm{E}\left[e^{Y_{x^f,t^f-1}(1) - W_{x^f,t^f-1}(1)} \,\middle|\, \mathcal{F}_0\right]}{\mathrm{E}\left[e^{Y_{x^f,t^f-1}(1) - W_{x^f,t^f-1}(1)} \left(\frac{\partial \kappa_{t^f}}{\partial h_0}\right) \,\middle|\, \mathcal{F}_0\right]},$$

In the fraction on the right side of the above equation, the only difference between the denominator and numerator is $\partial \kappa_{t^f} / \partial h_0$, which of course depends heavily on t^f. Compared with Equation (19), β_{x^f} no longer appears as a coefficient of the expectation in the denominator, offering an explanation to why the delta/vega ratio is relatively less sensitive to x^f. As a consequence, for the chosen times to maturity (5 and 15 years), all reference age combinations meet the necessary condition specified by (18), offering a reason as to why the effectiveness of a delta-vega hedge is fairly robust relative to the q-forwards' reference ages.

5.4.3 The Impact of the Time-to-Maturity Combinations

We now fix the reference ages to $x_1^f = 80$ and $x_2^f = 89$, and examine how the hedge effectiveness may vary with the q-forwards' times to maturity.[3] The hedging results are presented in Figure 13.

Except when both times to maturity are high, the delta-gamma hedges are almost as effective as their corresponding ex post optimal hedges for all time-to-maturity combinations. We can attribute this outcome to the property that the delta/gamma ratio of a q-forward is sensitive to its reference age but not to its time to maturity. The implication of this property can be observed from the left panel of Figure 14, which shows that when the reference ages are fixed to 80 and 89, the necessary condition specified by (18) is met no matter what times to maturity are chosen. The delta-gamma hedges do not perform well when both times to maturity are high, because in this case, the deltas and gammas of both q-forwards are very small (see Figures 5 and 6), so that the matrix on the left side of equation (15) is close to singular.

[3]When considering delta-gamma hedges with $t_1^f = 5$ and $t_2^f = 15$, these two reference ages result in the highest level of hedge effectiveness. Other reference ages may also be used in this analysis, provided that one of them is

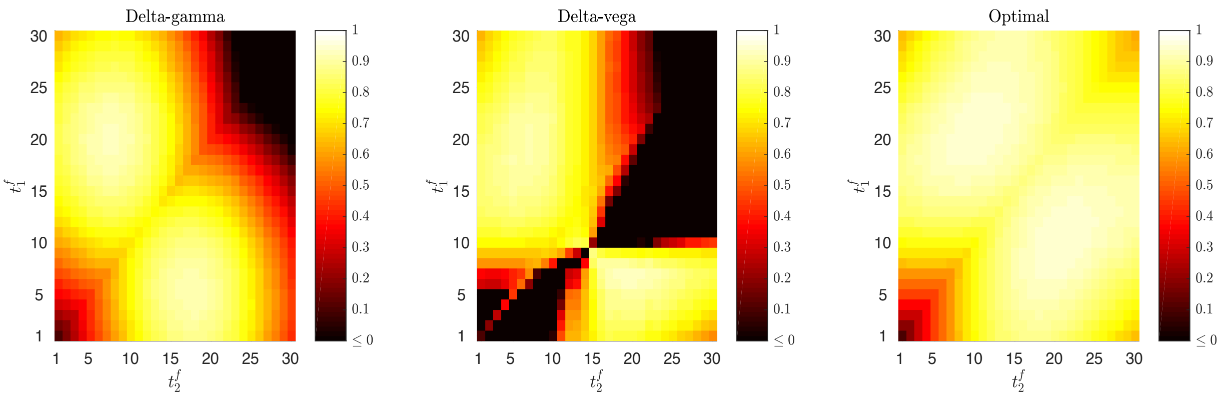

Fig. 13. Values of HE for the Delta-Gamma Hedges (Left), Delta-Vega Hedges (Center) and Ex Post Optimal Hedges (Right) with $\mathcal{J} = 2$ *q*-Forwards, $x_1^f = 80$, $x_2^f = 89$, $t_1^f, t_2^f = 1, \ldots, 30$

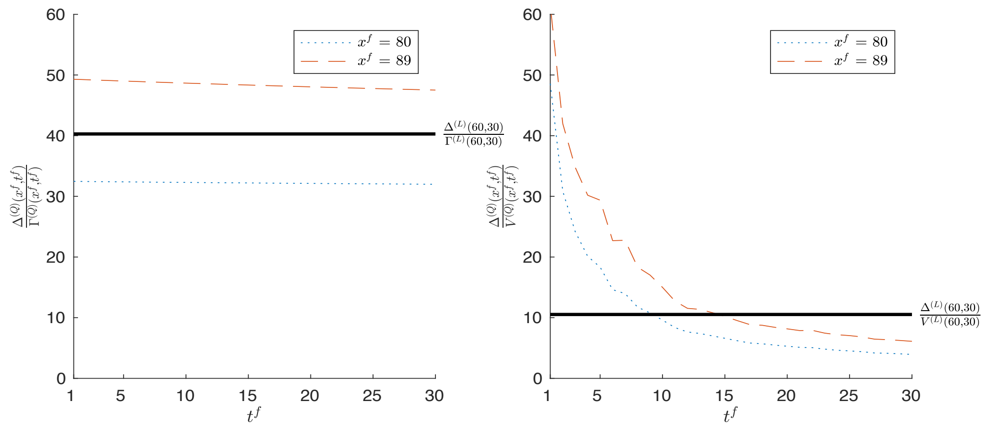

Fig. 14. Delta-Gamma (Left) and Delta-Vega (Right) Ratios for *q*-Forwards With $x^f = 80, 89$ and $t^f = 1, \ldots, 30$

Note: The solid horizontal line in the left (right) panel represents the delta-gamma (delta-vega) ratio for the liability being hedged.

On the other hand, the delta-vega hedges perform well for only some time-to-maturity combinations. This outcome can be explained by considering the property that the delta/vega ratio of a q-forward is sensitive to its time to maturity but not so much to its reference age. Because of this property, from Figure 14 we observe that in order to satisfy the necessary condition specified by (18), when the q-forward with $x^f = 80$ has a time to maturity of less than 10 years, the other q-forward (with $x^f = 89$) must have a time to maturity of greater than 15 years. Likewise, when the q-forward with $x^f = 89$ has a time to maturity of less than 15 years, the other q-forward (with $x^f = 80$) must have a time to maturity of greater than 10 years. It is noteworthy that part of the diagonal in the middle panel of Figure 13 is fairly bright. This results because, as previously mentioned, the necessary condition specified by (18) does not apply when the two q-forwards have identical times to maturity.

---

less than or equal to 86 and the other is greater than 86.

6 Validation With a Model-Free Approach

In Section 5, the model used to generate the evaluation scenarios is identical to the model from which the longevity Greeks are derived. We now examine how the hedging results may change when the model assumptions are waived in the evaluation work. To this end, we employ the nonparametric (model-free) bootstrapping method that was considered by Li and Ng (2011). The method is implemented as follows:

1. Calculate the historical mortality reduction rates, defined as
$$r_{x,t} = \frac{m_{x,t+1}}{m_{x,t}}.$$
Since we have 91 years of data, 90 values of $r_{x,t}$ are obtained for each age. The augmented Dickey-Fuller test is performed to confirm that the trend of $r_{x,t}$ over time at every age is weakly stationary.

2. Construct vectors of historical mortality improvement rates, i.e.,
$$\mathbf{r}_t = (r_{60,t}, \ldots, r_{89,t})'$$
for $t = 1921, \ldots, 2010$. The vectorization is performed to preserve any potential correlation across the age dimension.

3. To retain the potential serial dependence, $\mathbf{r}_t$ for $t = 1921, \ldots, 2010$ are grouped into overlapping blocks of size 2. The following 89 blocks are obtained:
$$(\mathbf{r}_{1921}, \mathbf{r}_{1922}),\ (\mathbf{r}_{1922}, \mathbf{r}_{1923}),\ \ldots,\ (\mathbf{r}_{2008}, \mathbf{r}_{2009}),\ (\mathbf{r}_{2009}, \mathbf{r}_{2010}).$$
The same block size was also used by Li and Ng (2011). We have considered other block sizes, which lead to similar conclusions.

4. A pseudo sample of reduction rates is obtained by drawing randomly from the 89 blocks in the previous step with replacement and pasting the blocks drawn end to end. The pseudo sample of reduction rates is multiplied by the most recent central death rates ($m_{x,2011}; x = 60, \ldots, 89$) to form a simulated mortality scenario.

5. Repeat the previous step 10,000 times to obtain 10,000 simulated mortality scenarios, which give 10,000 realizations of $\mathcal{L}(60, 30)|\mathcal{F}_0$ and $\mathcal{Q}(x^f, t^f)|\mathcal{F}_0$ for $x^f = 60, \ldots, 89$ and $t^f = 1, \ldots, 30$. The realizations of $\mathcal{L}(60, 30)|\mathcal{F}_0$ and $\mathcal{Q}(x^f, t^f)|\mathcal{F}_0$ allow us to estimate the effectiveness of the Greek hedges using Equation (10). They also permit us to derive the ex post optimal (variance-minimizing) hedges. Note that the longevity Greeks (and hence the notional amounts in the Greek hedges) are still calculated from the Lee-Carter model with GARCH effects.

Figure 15 shows the effectiveness of various hedges, estimated using the nonparametric bootstrapping method. As expected, the effectiveness of all hedges is reduced as the model assumptions are waived.

Let us first focus on the top row, where the effectiveness of the single Greek hedges is presented. Still, the delta and vega hedges can perform comparably to the ex post optimal hedges, provided that the q-forward's time to maturity is appropriately selected. The vega hedges are almost as effective as the ex post optimal hedges if the q-forward's time to maturity is longer than 10 years, whereas the delta hedges perform similarly to the ex post optimal hedges only if a short-dated q-forward is used. These observations are in line with the those made in Section 5.3.

When both the evaluation scenarios and the longevity Greeks are obtained from our assumed model, which implies that the log mortality rates at a given time point are perfectly correlated across ages, the effectiveness of the single Greek hedges is robust relative to the q-forward's reference age (see Figure 9). When the evaluation scenarios are obtained from the nonparametric bootstrap, the assumption of perfect age correlation no longer holds, so we observe that the robustness with respect to the choice of reference ages is weakened. For both delta and vega hedges, the nonparametrically estimated hedge effectiveness increases and then decreases with the q-forward's reference age. This pattern may be explained by considering the

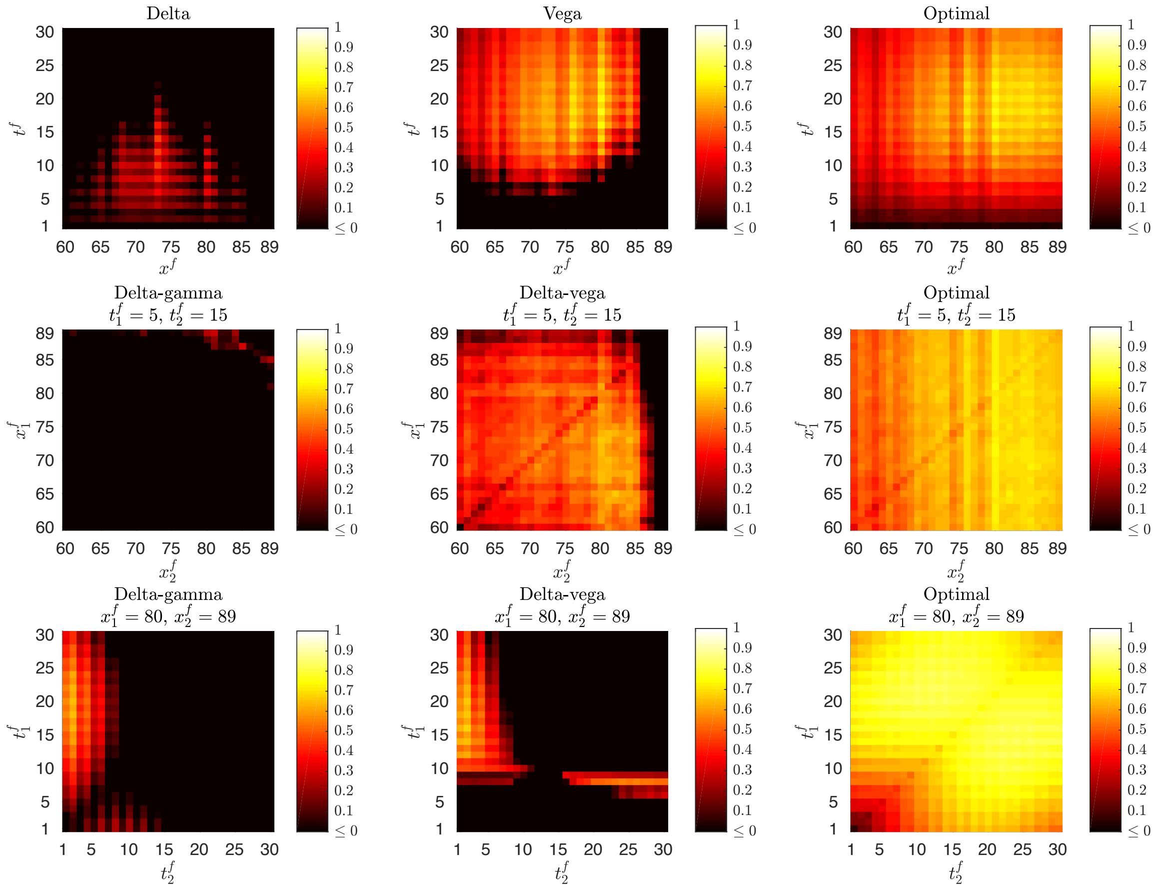

Fig. 15. Values of HE Produced by the Delta, Vega, Delta-Gamma, Delta-Vega and Ex Post Optimal Hedges for Different Choices of Reference Age(s) and Time(s) to Maturity

Note: All HE values are calculated using the nonparametric bootstrapping method with a block size of 2.

age-specific goodness of fit produced by the Lee-Carter model, which can be measured by the following explanation ratio:

$$\text{ER}(x) = 1 - \frac{\sum_t (\ln(m_{x,t}) - \alpha_x - \beta_x \kappa_t)^2}{\sum_t (\ln(m_{x,t}) - \alpha_x)^2},$$

where the summations are taken over the entire sample period.[4] The model gives a better fit to age x than age y if $\text{ER}(x)$ is greater than $\text{ER}(y)$. As shown in Figure 16, the estimated values of $\text{ER}(x)$ suggest that the Lee-Carter model gives a poorer fit at the ends of the age range. As a consequence, the sensitivity measures for a q-forward tend to be more inaccurate when its reference age is too high or low. The inaccuracy in turn leads to a low hedge effectiveness.

Next, we turn to the middle row of Figure 15, which displays the nonparametrically calculated HE values for the hedges with two q-forwards, of which the times to maturity are fixed to 5 and 15 years and the reference ages are allowed to vary from 60 to 89. The major conclusions drawn in Section 5.4.2 are still preserved even when the evaluation scenarios are generated using a model-free approach: (i) the delta-gamma hedges do not give a satisfactory performance for most combination of reference ages (that lead to one negative and one positive notional amount); (ii) compared with a delta-vega hedge, a delta-vega hedge is much more robust with respect to the choice of reference ages.

[4]This metric is adopted from the (non-age-specific) explanation ratio considered by Li and Lee (2005).

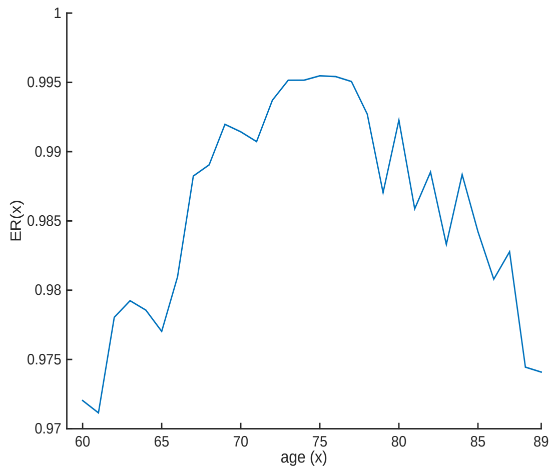

Fig. 16. Explanation Ratio ER(x) **for** $x = 60, \ldots, 89$

Finally, we study the bottom row of Figure 15, which displays the nonparametrically calculated HE values for the hedges with two q-forwards, of which the reference ages are fixed to 80 and 89 and the reference ages are allowed to vary from 1 to 30 years. The key conclusions drawn in Section 5.4.3 can still be observed: (i) the delta-vega hedges perform satisfactorily only for some time-to-maturity combinations; (ii) delta-gamma hedges do not work well only when the q-forwards' times to maturity are long.

7 Concluding Remarks

In this paper, we consider three longevity Greeks which enable us to calibrate an index-based longevity hedge. Most notably, we propose the longevity vega to address the empirical fact that for many populations, the volatility of mortality improvement rates changes stochastically over time. Semi-analytical formulas for the longevity Greeks of a q-forward and a stylized pension plan are provided.

The properties of the three longevity Greeks for q-forwards are studied. It is found that, for example, while the magnitudes of the longevity delta and gamma reduce with the time to maturity, the magnitude of the longevity vega increases and then decreases with the time to maturity. All of these properties can be explained by considering (i) the gradient and concavity of the curve of $\exp(-\exp(Y_{x,t}(1)))$ against $Y_{x,t}(1)$, (ii) the magnitude and variability of $Y_{x,t}(1)$, (iii) the pattern of β_x across age, and (iv) the time value of money.

We construct static hedges by matching one or two longevity Greeks, and examine how the performance of the Greek hedges may vary with the reference age(s) and time(s) to maturity of the q-forward(s) used. For instance, when matching one longevity Greek (with one q-forward), the hedge effectiveness is highly sensitive to the q-forward's time to maturity but not so to the q-forward's reference age. Specifically, a delta hedge performs satisfactorily only when the time to maturity is short, whereas a vega hedge behaves in the opposite way. This finding may help hedgers decide which longevity Greek to use when a q-forward with a certain specification is available to them.

We fully acknowledge that the longevity Greeks are model dependent. If another stochastic mortality model such as the Cairns-Blake-Dowd model (Cairns et al. 2006) is assumed, then the expressions for the longevity Greeks would become quite different. To address this problem, we validate our Greek hedges using the nonparametric bootstrapping method, which does not depend on any model. As expected, the hedge effectiveness estimated using the model-free approach is not as good as that estimated using the model from which the longevity Greeks are derived. Nevertheless, many of the points we made concerning the relationship between hedge effectiveness and q-forward specifications are still observed even when the evaluation scenarios are generated by a model-free approach.

We conclude this paper with a discussion of its caveats. First, the existence of stochastic volatility (and hence the necessity of the longevity vega) is data dependent. For some populations, particularly those with little historical mortality data, conditional heteroskedasticity may not be statistically significant. Second, we focus on q-forwards only and paid no attention to other mortality-linked securities such as S-forwards and longevity bonds. While the longevity Greeks for these more complex securities can be derived, their properties may not be easily explained using simple arguments. Finally, we disregard population basis risk and small sample risk, which can be taken into account in future research by using a multi-population mortality model and a death count process, respectively.

References

Brouhns, N., Denuit, M., and Van Keilegom, I. (2005). Bootstrapping the Poisson Log-Bilinear Model for Mortality Forecasting. *Scandinavian Actuarial Journal*, 2005(3):212–224.

Brouhns, N., Denuit, M., and Vermunt, J. K. (2002). A Poisson Log-Bilinear Regression Approach to the Construction of Projected Lifetables. *Insurance: Mathematics and Economics*, 31(3):373–393.

Cairns, A. J. G. (2011). Modelling and Management of Longevity Risk: Approximations to Survivor Functions and Dynamic Hedging. *Insurance: Mathematics and Economics*, 49(3):438–453.

Cairns, A. J. G. (2013). Robust Hedging of Longevity Risk. *Journal of Risk and Insurance*, 80(3):621–648.

Cairns, A. J. G., Blake, D., and Dowd, K. (2006). A Two-Factor Model for Stochastic Mortality with Parameter Uncertainty: Theory and Calibration. *Journal of Risk and Insurance*, 73(4):687–718.

Cairns, A. J. G., Dowd, K., Blake, D., and Coughlan, G. D. (2014). Longevity Hedge Effectiveness: A Decomposition. *Quantitative Finance*, 14(2):217–235.

Chai, C. M. H., Siu, T. K., Zhou, X., Hui, M., Chai, C. M. H., Kuen, T., and Xian, S. (2013). A Double-Exponential GARCH Model for Stochastic Mortality. *European Actuarial Journal*, 3(2):385–406.

Chen, H., MacMinn, R., and Sun, T. (2015). Multi-population Mortality Models: A Factor Copula Approach. *Insurance: Mathematics and Economics*, 63:135–146.

Coughlan, G. D. (2009). Longevity Risk Transfer: Indices and Capital Market Solutions. *The Handbook of Insurance-Linked Securities*, pages 261–281.

Coughlan, G. D., Epstein, D., Ong, A., Sinha, A., Hevia-Portocarrero, J., Gingrich, E., Khalaf-Allah, M., and Joseph, P. (2007). LifeMetrics: A Toolkit for Measuring and Managing Longevity and Mortality Risks.

Coughlan, G. D., Khalaf-Allah, M., Ye, Y., Kumar, S., Cairns, A. J. G., Blake, D., and Dowd, K. (2011). Longevity Hedging 101. *North American Actuarial Journal*, 15(2):150–176.

Crépey, S. (2004). Delta-Hedging Vega Risk? *Quantitative Finance*, 4(5):559–579.

Dahl, M., Glar, S., and Møller, T. (2011). Mixed Dynamic and Static Risk-Minimization With an Application to Survivor Wwaps. *European Actuarial Journal*, 1(S2):233–260.

Dahl, M., Melchior, M., and Møller, T. (2008). On Systematic Mortality Risk and Risk-Minimization With Survivor Swaps. *Scandinavian Actuarial Journal*, 2008(2-3):114–146.

Dahl, M. and Møller, T. (2006). Valuation and Hedging of Life Insurance Liabilities With Systematic Mortality Risk. *Insurance: Mathematics and Economics*, 39(2):193–217.

Engle, R. F. and Rosenberg, J. V. (1995). GARCH Gamma. *Journal of Derivatives*, 2(4):47–59.

Engle, R. F. and Rosenberg, J. V. (2000). Testing the Volatility Term Structure Using Option Hedging Criteria. *Journal of Derivatives*, 8(1):10–28.

Gao, Q. and Hu, C. (2009). Dynamic Mortality Factor Model With Conditional Heteroskedasticity. *Insurance: Mathematics and Economics*, 45(3):410–423.

Giacometti, R., Bertocchi, M., Rachev, S. T., and Fabozzi, F. J. (2012). A Comparison of the Lee-Carter Model and AR-ARCH Model for Forecasting Mortality Rates. *Insurance: Mathematics and Economics*, 50(1):85–93.

Graziani, G. (2014). Longevity Risk: A Fine Balance. *Institutional Investor Journals: Special Issue on Pension and Longevity Risk Transfer for Institutional Investors*, 2014(1):35–37.

Javaheri, A., Wilmott, P., and Haug, E. G. (2004). GARCH and Volatility Swaps. *Quantitative Finance*, 4(5):589–595.

Koissi, M. C., Shapiro, A. F., and Hognas, G. (2006). Evaluating and Extending the Lee-Carter Model for Mortality Forecasting: Bootstrap Confidence Interval. *Insurance: Mathematics and Economics*, 38(1):1–20.

Lee, R. and Miller, T. (2001). Evaluating the Performance of the Lee-Carter Method for Forecasting Mortality. *Demography*, 38(4):537–549.

Lee, R. D. and Carter, L. R. (1992). Modeling and Forecasting U.S. Mortality. *Journal of the American Statistical Association*, 87(419):659–671.

Lehar, A., Scheicher, M., and Schittenkopf, C. (2002). GARCH vs Stochastic Volatility: Option Pricing and Risk Management. *Journal of Banking & Finance*, 26:323–345.

Li, J. (2014). A Quantitative Comparison of Simulation Strategies for Mortality Projection. *Annals of Actuarial Science*, 8(2):281–297.

Li, J. S.-H. and Hardy, M. R. (2011). Measuring Basis Risk in Longevity Hedges. *North American Actuarial Journal*, 15(2):177–200.

Li, J. S.-H. and Luo, A. (2012). Key q-Duration: A Framework for Hedging Longveity Risk. *ASTIN Bulletin*, 42(2):413–452.

Li, J. S.-H. and Ng, A. C.-Y. (2011). Canonical Valuation of Mortality-Linked Securities. *Journal of Risk and Insurance*, 78(4):853–884.

Li, N. and Lee, R. (2005). Coherent Mortality Forecasts for a Group of Populations: An Extension of the Lee-Carter Method. *Demography*, 42(3):575–594.

Lin, T. and Tsai, C. C. L. (2013). On the Mortality/Longevity Risk Hedging With Mortality Immunization. *Insurance: Mathematics and Economics*, 53(3):580–596.

Lin, T. and Tsai, C. C.-L. (2014). Applications of Mortality Durations and Convexities in Natural Hedges. *North American Actuarial Journal*, 18(3):417–442.

Liu, X. and Braun, W. J. (2010). Investigating Mortality Uncertainty Using the Block Bootstrap. *Journal of Probability and Statistics*, 2010.

Luciano, E. and Regis, L. (2014). Efficient Versus Inefficient Hedging Strategies in the Presence of Financial and Longevity (Value at) Risk. *Insurance: Mathematics and Economics*, 55(1):68–77.

Luciano, E., Regis, L., and Vigna, E. (2012). Delta-Gamma Hedging of Mortality and Interest Rate Risk. *Insurance: Mathematics and Economics*, 50(3):402–412.

Luciano, E., Regis, L., and Vigna, E. (2015). Single- and Cross-Generation Natural Hedging of Longevity and Financial Risk. *Journal of Risk and Insurance*.

McDonald, R. L. (2012). *Derivatives Markets*. Pearson Boston.

Michaelson, A. and Mulholland, J. (2014). Strategy for Increasing the Global Capacity for Longevity Risk Transfer: Developing Transactions That Attract Capital Markets Investors. *Journal of Alternative Investments*, 17(1):18–27.

Ngai, A. and Sherris, M. (2011). Longevity Risk Management for Life and Variable Annuities: The Effectiveness of Static Hedging Using Longevity Bonds and Derivatives. *Insurance: Mathematics and Economics*, 49(1):100–114.

Plat, R. (2011). One-Year Value-at-Risk for Longevity and Mortality. *Insurance: Mathematics and Economics*, 49(3):462–470.

Renshaw, A. E. and Haberman, S. (2008). On Simulation-Based Approaches to Risk Measurement in Mortality With Specific Reference to Poisson Lee-Carter Modelling. *Insurance: Mathematics and Economics*, 42(2):797–816.

Rosa, C. D., Luciano, E., and Regis, L. (2016). Basis Risk in Static Versus Dynamic Longevity-Risk Hedging. *Scandinavian Actuarial Journal*, pages 1–23.

Tsai, C. C. L. and Chung, S. L. (2013). Actuarial Applications of the Linear Hazard Transform in Mortality Immunization. *Insurance: Mathematics and Economics*, 53(1):48–63.

Tsai, C. C.-L. and Jiang, L. (2011). Actuarial Applications of the Linear Hazard Transform in Life Contingencies. *Insurance: Mathematics and Economics*, 49(1):70–80.

Tsai, J. T., Wang, J. L., and Tzeng, L. Y. (2010). On the Optimal Product Mix in Life Insurance Companies Using Conditional Value at Risk. *Insurance: Mathematics and Economics*, 46(1):235–241.

Tsay, R. S. (2005). *Analysis of Financial Time Series*. John Wiley & Sons.

Wang, J. L., Huang, H. C., Yang, S. S., and Tsai, J. T. (2010). An Optimal Product Mix for Hedging Longevity Risk in Life Insurance Companies: The Immunization Theory Approach. *Journal of Risk and Insurance*, 77(2):473–497.

Wang, Z. and Li, J. S.-H. (2016). A DCC-GARCH Multi-population Mortality Model and Its Applications to Pricing Catastrophic Mortality Bonds. *Finance Research Letters*, 16:103–111.

Wong, T. W., Chiu, M. C., and Wong, H. Y. (2014). Time-Consistent Mean-Variance Hedging of Longevity Risk: Effect of Cointegration. *Insurance: Mathematics and Economics*, 56:56–67.

Yang, B., Li, J., and Balasooriya, U. (2015). Using Bootstrapping to Incorporate Model Error for Risk-Neutral Pricing of Longevity Risk. *Insurance: Mathematics and Economics*, 62:16–27.

Zhou, K. Q. and Li, J. S.-H. (2016). Dynamic Longevity Hedging in the Presence of Population Basis Risk: A Feasibility Analysis from Technical and Economic Perspectives. *Journal of Risk and Insurance*.

Appendix A Derivation of the Longevity Greeks

This appendix presents the derivations of the three longevity Greeks for $p_{x,t}(T, \kappa_0, h_0)$. In all derivations, it is assumed that the expectation and differential operator are interchangeable.

- The longevity delta for $p_{x,t}(T, \kappa_0, h_0)$:

$$\begin{aligned}\Delta_{x,t}(T) = \frac{\partial p_{x,t}(T, \kappa_0, h_0)}{\partial \kappa_0} &= \frac{\partial}{\partial \kappa_0} \mathrm{E}\left[e^{-W_{x,t}(T)} \,\middle|\, \mathcal{F}_0 \right] = \mathrm{E}\left[e^{-W_{x,t}(T)} \left(-\frac{\partial}{\partial \kappa_0} W_{x,t}(T) \right) \,\middle|\, \mathcal{F}_0 \right] \\ &= \mathrm{E}\left[e^{-W_{x,t}(T)} \left(-\sum_{s=1}^{T} e^{Y_{x,t}(s)} \left(\frac{\partial}{\partial \kappa_0} Y_{x,t}(s) \right) \right) \,\middle|\, \mathcal{F}_0 \right] \\ &= -\sum_{s=1}^{T} \beta_{x+s-1} \,\mathrm{E}\left[e^{Y_{x,t}(s) - W_{x,t}(T)} \,\middle|\, \mathcal{F}_0 \right].\end{aligned}$$

- The longevity gamma for $p_{x,t}(T, \kappa_0, h_0)$:

$$\begin{aligned}\Gamma_{x,t}(T) = \frac{\partial^2 p_{x,t}(T, \kappa_0, h_0)}{\partial \kappa_0^2} &= \frac{\partial}{\partial \kappa_0} \left(\frac{\partial p_{x,t}(T, \kappa_0, h_0)}{\partial \kappa_0} \right) = \frac{\partial}{\partial \kappa_0} \left(\mathrm{E}\left[-\sum_{s=1}^{T} \beta_{x+s-1} e^{Y_{x,t}(s) - W_{x,t}(T)} \,\middle|\, \mathcal{F}_0 \right] \right) \\ &= \mathrm{E}\left[-\sum_{s=1}^{T} \beta_{x+s-1} e^{Y_{x,t}(s) - W_{x,t}(T)} \frac{\partial}{\partial \kappa_0} (Y_{x,t}(s) - W_{x,t}(T)) \,\middle|\, \mathcal{F}_0 \right] \\ &= \mathrm{E}\left[-\sum_{s=1}^{T} \beta_{x+s-1} e^{Y_{x,t}(s) - W_{x,t}(T)} \left(\beta_{x+s-1} - \sum_{u=1}^{T} \beta_{x+u-1} e^{Y_{x,t}(u)} \right) \,\middle|\, \mathcal{F}_0 \right] \\ &= \mathrm{E}\left[e^{-W_{x,t}(T)} \left(\left(\sum_{s=1}^{T} \beta_{x+s-1} e^{Y_{x,t}(s)} \right)^2 - \sum_{s=1}^{T} \beta_{x+s-1}^2 e^{Y_{x,t}(s)} \right) \,\middle|\, \mathcal{F}_0 \right].\end{aligned}$$

- The longevity vega for $p_{x,t}(T, \kappa_0, h_0)$:

$$\begin{aligned}V_{x,t}(T) = \frac{\partial p_{x,t}(T, \kappa_0, h_0)}{\partial h_0} &= \mathrm{E}\left[e^{-W_{x,t}(T)} \left(-\sum_{s=1}^{T} e^{Y_{x,t}(s)} \left(\frac{\partial}{\partial h_0} Y_{x,t}(s) \right) \right) \,\middle|\, \mathcal{F}_0 \right] \\ &= \mathrm{E}\left[e^{-W_{x,t}(T)} \left(-\sum_{s=1}^{T} e^{Y_{x,t}(s)} \left(\beta_{x+s-1} \frac{\partial \kappa_{t+s}}{\partial h_0} \right) \right) \,\middle|\, \mathcal{F}_0 \right] \\ &= -\sum_{s=1}^{T} \beta_{x+s-1} \,\mathrm{E}\left[e^{Y_{x,t}(s) - W_{x,t}(T)} \left(\frac{\partial \kappa_{t+s}}{\partial h_0} \right) \,\middle|\, \mathcal{F}_0 \right],\end{aligned}$$

where

$$\frac{\partial \kappa_{t+s}}{\partial h_0} = \sum_{u=1}^{t+s} \frac{\eta_u}{2\sqrt{h_u}} \frac{\partial h_u}{\partial h_0}$$

and

$$\frac{\partial h_u}{\partial h_0} = \begin{cases} b \prod_{v=1}^{u-1} (a\eta_{u-v}^2 + b) & \text{if } u \geq 2 \\ b & \text{if } u = 1 \end{cases}.$$

Appendix B Proof of Theorem 1

For convenience, we let $\mathrm{E}_t[\cdot] := \mathrm{E}_t[\cdot|\mathcal{F}_t]$. Because $\eta_t \overset{i.i.d.}{\sim} N(0,1)$, we have $\mathrm{E}_{t-1}[\eta_t] = 0$, $\mathrm{E}_{t-1}[\eta_t^2] = 1$, $\mathrm{E}_{t-1}[\eta_t^3] = 0$, and $\mathrm{E}_{t-1}[\eta_t^4] = 3$ for $t \geq 1$. These results are used in this and the following appendixes.

Proof of Theorem 1. For $t^f = 1$,

$$\mathrm{E}_0\left[\left(\sqrt{h_1} \eta_1 \right)^2 \right] = \omega + a\epsilon_0 + bh_0 = z_{1,0} + z_{1,1} h_0,$$

where $z_{1,0} = \omega + a\epsilon_0$ and $z_{1,1} = b$ do not depend on h_0. Thus, Equation (12) holds for $t^f = 1$. Let $t > 1$ be given, and suppose that Equation (12) holds for $t^f = t - 1$. Then, for $t^f = t$,

$$\begin{aligned}
\mathrm{E}_0\left[\left(\sum_{s=1}^{t}\sqrt{h_s}\eta_s\right)^2\right] &= \mathrm{E}_0\left[\left(\sum_{s=1}^{t-1}\sqrt{h_s}\eta_s + \sqrt{h_t}\eta_t\right)^2\right] \\
&= \mathrm{E}_0\left[\left(\sum_{s=1}^{t-1}\sqrt{h_s}\eta_s\right)^2\right] + \mathrm{E}_0\left[h_t\right] \\
&= z_{t-1,0} + z_{t-1,1}h_0 + \left(\frac{\omega - \omega(a+b)^t}{1-a-b}\right) + (a+b)^{t-1}(a\epsilon_0^2 + bh_0) \\
&= z_{t-1,0} + \left(\frac{\omega - \omega(a+b)^t}{1-a-b} + a(a+b)^{t-1}\epsilon_0^2\right) + \left(z_{t-1,1} + b(a+b)^{t-1}\right)h_0 \\
&= z_{t,0} + z_{t,1}h_0,
\end{aligned}$$

where $z_{t,0}$ and $z_{t,1}$ do not depend on h_0. Hence, Equation (12) also holds for $t^f = t$. By the principle of induction, Equation (12) holds for $t^f \geq 1$. $\square$

Appendix C Proof of Theorem 2

To prove Theorem 2, we need the following lemma.

Lemma 4. *For $t^f \geq 2$,*

$$\mathrm{E}_0\left[\left(\sum_{s=1}^{t^f-1}\sqrt{h_s}\eta_s\right)h_{t^f}\right] = 0. \tag{C.1}$$

Proof of Lemma 4. For $t^f = 2$,

$$\mathrm{E}_0\left[\sqrt{h_1}\eta_1 h_2\right] = \sqrt{h_1}\mathrm{E}_0\left[\eta_1\right]h_2 = 0.$$

Thus, Equation (C.1) holds for $t^f = 2$. Let $t > 2$ be given, and suppose Equation (C.1) holds for $t^f = t-1$. Then, for $t^f = t$,

$$\begin{aligned}
\mathrm{E}_0\left[\left(\sum_{s=1}^{t-1}\sqrt{h_s}\eta_s\right)h_t\right] &= \mathrm{E}_0\left[\left(\sum_{s=1}^{t-2}\sqrt{h_s}\eta_s + \sqrt{h_{t-1}}\eta_{t-1}\right)\left(\omega + \left(a\eta_{t-1}^2 + b\right)h_{t-1}\right)\right] \\
&= \mathrm{E}_0\left[\left(\sum_{s=1}^{t-2}\sqrt{h_s}\eta_s\right)h_{t-1}\right](a+b) \\
&= 0.
\end{aligned}$$

So Equation (C.1) also holds for $t^f = t$. By the principle of induction, Equation (C.1) holds for $t^f \geq 2$. $\square$

Proof of Theorem 2. For $t^f = 1$,

$$\mathrm{E}_0\left[\left(\sqrt{h_1}\eta_1\right)^3\right] = h_1^{\frac{3}{2}}\mathrm{E}_0\left[\eta_1^3\right] = 0.$$

Thus, Equation (13) holds for $t^f = 1$. Let $t > 1$ be given, and suppose Equation (13) holds for $t^f = t - 1$.

Then, for $t^f = t$,

$$\begin{aligned}
\mathrm{E}_0\left[\left(\sum_{s=1}^{t}\sqrt{h_s}\eta_s\right)^3\right] &= \mathrm{E}_0\left[\left(\sum_{s=1}^{t-1}\sqrt{h_s}\eta_s + \sqrt{h_t}\eta_t\right)^3\right] \\
&= \mathrm{E}_0\left[\left(\sum_{s=1}^{t-1}\sqrt{h_s}\eta_s\right)^3\right] + 3\mathrm{E}_0\left[\left(\sum_{s=1}^{t-1}\sqrt{h_s}\eta_s\right)h_t\right] \\
&= 0,
\end{aligned}$$

since $\mathrm{E}_0\left[\left(\sum_{s=1}^{t-1}\sqrt{h_s}\eta_s\right)h_t\right] = 0$ by Lemma 4. Hence, Equation (13) also holds for $t^f = t$. By the principle of induction, Equation (13) holds for $t^f \geq 1$. □

Appendix D Proof of Theorem 3

To prove Theorem 3, we need the following two lemmas.

Lemma 5. *For $t^f \geq 1$,*

$$\mathrm{E}_0\left[h_{t^f}^2\right] = \phi_{t^f,0} + \phi_{t^f,1}h_0 + \phi_{t^f,2}h_0^2, \tag{D.1}$$

where $\phi_{t^f,0}$, $\phi_{t^f,1}$ and $\phi_{t^f,2}$ do not depend on h_0.

Proof of Lemma 5. For $t^f = 1$,

$$\mathrm{E}_0\left[h_1^2\right] = (\omega + a\epsilon_0^2)^2 + 2b(\omega + a\epsilon_0^2)h_0 + b^2h_0^2 = \phi_{1,0} + \phi_{1,1}h_0 + \phi_{1,2}h_0^2,$$

where $\phi_{1,0} = (\omega + a\epsilon_0^2)^2$, $\phi_{1,1} = 2b(\omega + a\epsilon_0^2)$ and $\phi_{1,2} = b^2$ do not depend on h_0. Hence, Equation (D.1) holds for $t^f = 1$. Let $t > 1$ be given, and suppose Equation (D.1) holds for $t^f = t - 1$. Then, for $t^f = t$,

$$\begin{aligned}
&\mathrm{E}_0\left[h_t^2\right] \\
&= \mathrm{E}_0\left[\left(\omega + \left(a\eta_{t-1}^2 + b\right)h_{t-1}\right)^2\right] \\
&= \mathrm{E}_0\left[\omega^2 + 2\omega(a+b)h_{t-1} + \left(3a^2 + 2ab + b^2\right)h_{t-1}^2\right] \\
&= \omega^2 + \pi_1\left(\frac{\omega - \omega(a+b)^{t-1}}{1-a-b} + (a+b)^{t-2}(a\epsilon_0^2 + bh_0)\right) + \pi_2\left(\phi_{t-1,0} + \phi_{t-1,1}h_0 + \phi_{t-1,2}h_0^2\right) \\
&= \pi_2\phi_{t-1,0} + \omega^2 + \frac{\pi_1\omega(1-(a+b)^{t-1})}{1-a-b} + \pi_1 a(a+b)^{t-2}\epsilon_0^2 + \left(\pi_2\phi_{t-1,1} + \pi_1 b(a+b)^{t-2}\right)h_0 + \pi_2\phi_{t-1,2}h_0^2 \\
&= \phi_{t,0} + \phi_{t,1}h_0 + \phi_{t,2}h_0^2,
\end{aligned}$$

where $\phi_{t,0}$, $\phi_{t,1}$ and $\phi_{t,2}$ do not depend on h_0, and $\pi_1 = 2\omega(a+b)$ and $\pi_2 = 3a^2+2ab+b^2$. Thus, Equation (D.1) also holds for $t^f = t$. By the principle of induction, Equation (D.1) holds for $t^f \geq 1$.

□

Lemma 6. *For $t^f \geq 2$,*

$$\mathrm{E}_0\left[\left(\sum_{s=1}^{t^f-1}\sqrt{h_s}\eta_s\right)^2 h_{t^f}\right] = \psi_{t^f,0} + \psi_{t^f,1}h_0 + \psi_{t^f,2}h_0^2, \tag{D.2}$$

where $\psi_{t^f,0}$, $\psi_{t^f,1}$ and $\psi_{t^f,2}$ do not depend on h_0.

Proof of Lemma 6. For $t^f = 2$,

$$\begin{aligned}
\mathrm{E}_0\left[\left(\sqrt{h_1}\eta_1\right)^2 h_2\right] &= \omega h_1 + (3a+b)h_1^2 \\
&= \left(\omega^2 + \omega a\epsilon_0^2 + (3a+b)(\omega + a\epsilon_0^2)^2\right) + \left(b\omega + 2b(3a+b)(\omega + a\epsilon_0^2)\right) h_0 + b^2(3a+b)h_0^2 \\
&= \psi_{2,0} + \psi_{2,1}h_0 + \psi_{2,2}h_0^2,
\end{aligned}$$

where $\psi_{2,0} = \omega^2 + \omega a\epsilon_0^2 + (3a+b)(\omega + a\epsilon_0^2)^2$, $\psi_{2,1} = b\omega + 2b(3a+b)(\omega + a\epsilon_0^2)$ and $\psi_{2,2} = b^2(3a+b)$ do not depend on h_0. Thus, Equation (D.2) holds for $t^f = 2$. Let $t > 2$ be given, and suppose Equation (D.2) holds for $t^f = t-1$. Then, for $t^f = t$,

$$\begin{aligned}
&\mathrm{E}_0\left[\left(\sum_{s=1}^{t-1}\sqrt{h_s}\eta_s\right)^2 h_t\right] \\
&= \mathrm{E}_0\left[\left(\sum_{s=1}^{t-2}\sqrt{h_s}\eta_s + \sqrt{h_{t-1}}\eta_{t-1}\right)^2 \left(\omega + (a\eta_{t-1}^2 + b)h_{t-1}\right)\right] \\
&= (a+b)\mathrm{E}_0\left[\left(\sum_{s=1}^{t-2}\sqrt{h_s}\eta_s\right)^2 h_{t-1}\right] + \omega\mathrm{E}_0\left[\left(\sum_{s=1}^{t-1}\sqrt{h_s}\eta_s\right)^2\right] + (3a+b)\mathrm{E}_0\left[h_{t-1}^2\right] \\
&= \left((a+b)\psi_{t-1,0} + (3a+b)\phi_{t-1,0} + \omega z_{t-1,0}\right) + \left((a+b)\psi_{t-1,1} + (3a+b)\phi_{t-1,1} + \omega z_{t-1,1}\right) h_0 \\
&\quad + \left((a+b)\psi_{t-1,2} + (3a+b)\phi_{t-1,2}\right) h_0^2 \\
&= \psi_{t,0} + \psi_{t,1}h_0 + \psi_{t,2}h_0^2,
\end{aligned}$$

where $\psi_{t,0}$, $\psi_{t,1}$ and $\psi_{t,2}$ do not depend on h_0. Hence, Equation (D.2) also holds for $t^f = t$. By the principle of induction, Equation (D.2) holds for $t^f \geq 2$. □

Proof of Theorem 3. For $t^f = 1$,

$$\begin{aligned}
\mathrm{E}_0\left[\left(\sqrt{h_1}\eta_1\right)^4\right] &= 3(\omega + a\epsilon_0^2)^2 + 6b(\omega + a\epsilon_0^2)h_0 + 3b^2h_0^2 \\
&= c_{1,0} + c_{1,1}h_0 + c_{1,2}h_0^2,
\end{aligned}$$

where $c_{1,0} = 3(\omega + a\epsilon_0^2)^2$, $c_{1,1} = 6b(\omega + a\epsilon_0^2)$ and $c_{1,2} = 3b^2$ do not depend on h_0. Thus, Equation (14) holds for $t^f = 1$. Let $t > 1$ be given, and suppose Equation (14) holds for $t^f = t-1$. Then, for $t^f = t$,

$$\begin{aligned}
\mathrm{E}_0\left[\left(\sum_{s=1}^{t}\sqrt{h_s}\eta_s\right)^4\right] &= \mathrm{E}_0\left[\left(\sum_{s=1}^{t-1}\sqrt{h_s}\eta_s + \sqrt{h_t}\eta_t\right)^4\right] \\
&= \mathrm{E}_0\left[\left(\sum_{s=1}^{t-1}\sqrt{h_s}\eta_s\right)^4\right] + 6\mathrm{E}_0\left[\left(\sum_{s=1}^{t-1}\sqrt{h_s}\eta_s\right)^2 h_t\right] + 3\mathrm{E}_0\left[h_t^2\right] \\
&= \left(c_{t-1,0} + 6\psi_{t,0} + 3\phi_{t,0}\right) + \left(c_{t-1,1} + 6\psi_{t,1} + 3\phi_{t,1}\right) h_0 + \left(c_{t-1,2} + 6\psi_{t,2} + 3\phi_{t,2}\right) h_0^2 \\
&= c_{t,0} + c_{t,1}h_0 + c_{t,2}h_0^2,
\end{aligned}$$

where $c_{t,0}$, $c_{t,1}$ and $c_{t,2}$ do not depend on h_0. Therefore, Equation (14) also holds for $t^f = t$. By the principle of induction, Equation (14) holds for $t^f \geq 1$. Furthermore, $z_{t^f,1}$ in Equation (12), $\phi_{t^f,1}$ and $\phi_{t^f,2}$

in Equation (D.1), and $\psi_{t^f,1}$ and $\psi_{t^f,2}$ in Equation (D.2) can be solved as follows:

$$
\begin{aligned}
z_{t^f,1} &= \frac{b - b(a+b)^{t_f}}{1-a-b}, \\
\phi_{t^f,1} &= \left(\frac{b\pi_1}{a+b-\pi_2}\right)(a+b)^{t^f-1} + \left(2b(\omega + a\epsilon_0^2) - \frac{b\pi_1}{a+b-\pi_2}\right)\pi_2^{t^f-1} = \pi_3(a+b)^{t^f-1} + \pi_4\pi_2^{t^f-1}, \\
\phi_{t^f,2} &= b^2\pi_2^{t^f-1}, \\
\psi_{t^f,1} &= \frac{\pi_4(3a+b)}{a+b-\pi_2}\left((a+b)^{t^f-1} - \pi_2^{t^f-1}\right) + \frac{b\omega}{(1-a-b)^2}\left(1-(a+b)^{t^f-1}\right) \\
&\quad + \left(\frac{2b\omega(3a+b)}{a+b-\pi_2} - \frac{b\omega}{1-a-b}\right)(a+b)^{t^f-1}(t^f-1), \\
\psi_{t^f,2} &= \frac{b^2(3a+b)}{a+b-\pi_2}\left((a+b)^{t^f-1} - \pi_2^{t^f-1}\right),
\end{aligned}
$$

where $\pi_3 = \frac{b\pi_1}{a+b-\pi_2}$ and $\pi_4 = 2b(\omega + a\epsilon_0^2) - \pi_3$. Substituting the expressions above into $c_{t^f,1}$ and $c_{t^f,2}$, we obtain

$$
\begin{aligned}
c_{t^f,1} = 6b(\omega + a\epsilon_0^2) &+ \left(\frac{6\pi_4(3a+b)}{a+b-\pi_2} - \frac{6b\omega}{(1-a-b)^2} + 3\pi_3\right)\left(\frac{a+b-(a+b)^{t^f}}{1-a-b}\right) \\
&+ 6\left(\frac{2b\omega(3a+b)}{a+b-\pi_2} - \frac{b\omega}{1-a-b}\right)\left(\frac{(a+b) - t^f(a+b)^{t^f} + (t^f-1)(a+b)^{t^f+1}}{(1-a-b)^2}\right) \\
&+ \left(3\pi_4 - \frac{6\pi_4(3a+b)}{a+b-\pi_2}\right)\left(\frac{\pi_2 - \pi_2^{t^f}}{1-\pi_2}\right) + \frac{6b\omega}{(1-a-b)^2}(t^f-1), \\
c_{t^f,2} = 3b^2 &+ \left(\frac{6b^2(3a+b)}{a+b-\pi_2}\right)\left(\frac{a+b-(a+b)^{t^f}}{1-a-b}\right) + \left(3b^2 - \frac{6b^2(3a+b)}{a+b-\pi_2}\right)\left(\frac{\pi_2 - \pi_2^{t^f}}{1-\pi_2}\right).
\end{aligned}
$$

It is clear that $c_{t^f,1}$ tends to ∞ as $t^f \to \infty$, and if $\pi_2 = 3a^2 + 2ab + b^2 < 1$, then $c_{t^f,2}$ tends to a constant as $t^f \to \infty$. $\square$